

RESEARCH

Open Access



Modelling innovation adoption spreading in complex networks

Jing-Lin Duanmu¹ and Wei Koong Chai^{2*}

*Correspondence:
wchai@bournemouth.ac.uk

¹ University of Exeter Business
School, Exeter EX4 4PU, UK

² Department of Computing
& Informatics, Bournemouth
University, Dorset BH12 5BB, UK

Abstract

Innovation adoption pattern has been found to be influenced by the underlying social network structure and its constituent entities. In this paper, we model innovation diffusion considering (1) the role of network structures in dictating the spread of adoption and (2) how individual's characteristic/capability influences the path of diffusion (e.g. an individual may have different attitude or ability towards adopting a new innovation). We consider that each individual is unique and his/her position in the network is important. We draw on the epidemic theory and model the diffusion dynamics via a continuous-time Markov chain which offers strong analytical tractability while retaining a high-level of generality. Our model allows derivation of individual's adoption probability and the aggregate adoption behavior of the network as a whole. Precise computation of individual adoption decision conditioned by the population's behavior is of exponential complexity (i.e., the state space exponentially increases with the size of the network). By applying a mean field approximation, the analysis complexity of the spreading mechanics is reduced from exponential ($O(5^N)$) to polynomial ($O(N)$) and thus allowing our approach to scale for large networks. We offer insights into how the network spectrum affects the innovation exposure rate and spreading of innovation individually and across communities with different adoption behaviors. We compare our model against a wide-range of Monte-Carlo experiments and show close agreements in different settings (including both homogeneous and heterogeneous population cases). Finally, we illustrate the effects of the embedded social structure and the characteristics of individuals in the network on the path of innovation diffusion via two use cases: (i) innovation adoption of EU countries in a Single Market Programme and (ii) innovation adoption of specific class of technology (specifically financial technologies (FinTech)).

Keywords: Innovation adoption, Complex networks, Continuous-time Markov Chain

Introduction

Innovation diffusion¹ has been the focus of various studies over the years and from different perspectives including economics, sociology, business and trade, marketing and statistical physics. One important determinant on the path of diffusion is the structure of the contact network (Acemoglu et al. 2007; Rogers 2003). The adoption decision of

¹ We use the word "innovation" as a generic term referring to any subject of adoption that is being disseminated in a network (e.g. new technologies or techniques, a social norm or practice (Morris et al. 2015; Olcina et al. 2018), a government or corporate policy (Dreiling and Darves 2011), abstract ideas or marketing strategies (Dinh et al. 2014).

an individual entity² has been found to be correlated with its social and business contacts (Young 2003) and thus, relies on exposures from its neighbors while concurrently, the decisions of the neighbors in turn are influenced by their respective neighbors. The spreading of an innovation is then heavily dependent on *who meets with whom and when*. A node having many (i.e., different sources of influence) and regular (i.e., continuous and persistent influence) contacts with others who have already adopted an innovation should intuitively be more likely to learn about the innovation and make an adoption decision earlier as compared to a node who does not have immediate contacts with adopters. For instance, Acemoglu et al. (2011) modeled diffusion paths in social networks based on multiple sources of adoption in neighborhood by extending the classical linear threshold model (Granovetter 1978) to a stochastic one. Another extension from (Granovetter 1978) is (Mili et al. 2018) in which the authors, in addition to the linear threshold model, added consideration on node preference by introducing a parameter characterizing the node profile. The work in this line of approach uses threshold(s) to determine whether a node adopt or not. On the other hand, Delre et al. (2007) proposed an epidemiological model for innovation diffusion explicitly considering heterogeneous consumer decision-making affected by social influences in his/her personal contact network. In line with this, various techniques from social and complex network analysis were also used. In Kali and Reyes (2007), the authors utilized a network approach to study international economic integration while Bhattacharya et al. (2008) analyzed the international trade network as a weighted network model. In Dreiling and Darves (2011), network analysis was used to look into how organizational and class cohesion affects trade policies. Meanwhile, Kinne (2012) exploited the concept of centrality to predict trades with dyadic trade-conflict relationships as oppose to large-scale trade integration. The process of globalization is linked with the small-world network effect in Duernecker and Vega-Redondo (2018) and the study showed how long bridging links decreases local saturation. On the other hand, Kim and Shin (2002) adopted a social network approach to argue that globalization and regionalization are not contradictory processes. Furthermore, community structures often exists in a network where groups of nodes exhibit similar properties (e.g. spatial network which has clear geographical boundaries). This effect has been modeled for the case of customary contract setting in Young and Burke (2001), offering an illustrative example via a hypothetical state on how regional customs form a compromise between fully uniform and differentiated contracts. In short, a node's interactions in a network are not homogeneous and are dictated by the structure of the network. Therefore, the position of a node in the network is important (Banerjee et al. 2013) and as highlighted in Borge-Holthoefler et al. (2013), the interdependency between local and global network influence in shaping adoption rates in the context of complex network is an area that requires further investigation.

The nodes in a real network are usually heterogeneous. For instance, Jackson and Lopez-Pintado (2013) studied innovation diffusion in a social network where nodes are distinguished by their types (e.g. race, gender, age, wealth). The heterogeneity may come

² An entity could represent an individual person, a firm or an organization in a business or social network depending on the context. These entities are represented as nodes in a network and so, hereinafter, we will use the term "node" to represent any entity that may potentially adopt an innovation.

in different forms. First, nodes may have different ability to adopt the innovation. In Acemoglu et al. (2007), the authors relate technology adoption with contractual incompleteness and technological complementarities. Firms may also have different organizational and communication channels that influence their adoption decisions. In Chen and Kamal (2016), the authors showed that the use of Internet-enabled communication technology has strong impact on foreign boundary decisions by multinational firms. The ability to take risks is another factor that can determine the final adoption decisions and Ambrus et al. (2014) modeled the risk-sharing between communities. In Bandiera and Rasul (2006), it is also found that the amount of information regarding a new innovation affects the adoption choices of each node. While the ability to adopt an innovation may vary depending on the settings, some heterogeneities are intrinsic to the nodes (Hofstede 2003). This is true even for those existing or operating within the same environment (Suriñach and et. al. 2009). These “personality traits” can similarly have significant effects on the potential of adoptions. Using prevalence of human diseases as an instrument, Fogli and Veldkamp (2012) study the effect of social structure on technology diffusion, exploiting the individualism index reported in Hofstede (2003) to separate characters of different nation. Considering different “player identities”, Tinn (2010) focuses on the willingness of entrepreneurs to invest in frontier technology. Finally, another dimension of heterogeneity relates to the link between nodes. The relationship between different pairs of nodes can vary. With this in mind, Koka et al. (1999) highlighted the role of close and enduring interaction as a catalyst to fostering trade partnerships. Meanwhile, Morris et al. (2015) studied the transmission of cultural practices based on social norms.

In this paper, we argue that each individual is unique (i.e., the question on *who* you are) and how this individual is connected in its social/business contact network (i.e., the question on *where* you are) is an important determinant on innovation adoption paths and collectively, they lead to distinct innovation diffusion dynamic. In line with this, we develop and present a tractable epidemic analysis framework that models the spreading dynamics of innovation adoption, i.e., $SA_{rc}A_{rs}IR$ (Susceptible - Aware Receptive - Aware Resistive - Infected - Removed), named following the convention of epidemic theory. Our model explicitly consider the period between first exposure to final adoption decision (“incubation” period) where one forms an attitude of either receptive or resistive towards the innovation. We take into account both the role of the network structure and the heterogeneity of the nodes in the network discussed above and advocate the use of epidemic theory which has been widely used to describe various spreading phenomena. Our model is based on a continuous-time Markov chain which incorporates the effect of network structure into the analysis and derive adoption probability of each node rather than an aggregate macroscopic prediction. Specifically, the entire network topology is taken as input to the model, allowing all the nodes in the network to be considered individually. Our model also allows the definition of different connection type/strength between any two nodes by using weighted network representation. Hence, in this paper, we contribute a novel model for innovation adoption spreading with inclusion of explicit states accounting for the period prior to adoption decision. Methodologically, by adopting an individual-based mean-field approximation in epidemic theory, our model is capable of computing the spreading dynamics taking into account heterogeneities of

connectivity (i.e., considering the detail structure of the network topology) and node (i.e., considering that nodes are different and links between node pair are also different).

The rest of the paper is organized as follows. Section "A model for innovation adoption spreading" describes the development of our $SA_{rc}A_{rs}IR$ model. Section "The role of network topology" investigates the role of different network topologies in influencing the spreading dynamics including the probability of each node in adopting an innovation in homogeneous population (i.e., all nodes in the network has the same affinity towards adopting a new innovation). Here, we study individual node in the network (Sect. "Individual node in a network"), the network as a whole (Sect. "Networks with different structural properties") and network with communities (Sect. "Networks with communities"). We then proceed to focus on heterogeneous case and extend our model in Sect. "Heterogeneous innovation adoption". We demonstrate the predictive capacity of our model in Sect. "Use cases" where we apply the $SA_{rc}A_{rs}IR$ model in two use cases. Section "Conclusions" concludes our work.

A model for innovation adoption spreading

Brief theoretical background and literature review

Originated from epidemiology in biology for studying disease spreading, epidemic theory is intrinsically suitable for modeling spreading phenomena which has been studied in various context such as contagious disease spread through population (Anderson and May 1991; Sahneh et al. 2012; Giordano et al. 2020; Liu et al. 2020), digital viruses and malware infections (Kephart and White 1993; Garetto et al. 2003), information spreading in communication networks (Chakrabarti et al. 2007; Vojnović et al. 2010), propagation of news, gossips and rumors in (online) social networks (Li et al. 2014) and promotions via viral marketing campaigns (Dinh et al. 2014). Historically, the approach began with curve-fitting approach which is pragmatic but has limited use since it does not explain the mechanism of spreading (Daley and Gani 1999). In 1700 s, deterministic modelling approaches were used with a large, fixed population. These early works consider homogeneous mixing based on the law of mass action where nodes have equal probability of being in contact with each other (Kermack and McKendrick 1927; Daley and Gani 1999). Since late 1800 s, stochastic modelling approach is adopted since spreading dynamics are inherently probabilistic and thus, discrete and continuous Markov chain methods began to gain attention.

In classical epidemic models, a disease is broken down into several distinct states (or stages) and each individual in the population must assume one and only one of these states at any given time. This is known as compartmentalization. In our case here, the "disease" is the novel innovation that is being diffused. Two basic but widely used models are the SIS and SIR models (Kermack and McKendrick 1927; Whittle 1955; Daley and Gani 1999) where the possible states are: (1) *Susceptible* (State *S*) for individuals who are uninfected but prone to infection, (2) *Infected* (State *I*) for individuals who are infected and thus infectious and (3) *Removed* (State *R*) for individuals who are immune to infections and not infectious.

In most epidemic models, the infection is passed from one individual to another via contacts which can be of different forms (e.g. business or trading relationship, social interactions, etc.). Essentially, this refers to the transition of states. However,

the contacts are usually modeled using constant transition rate which then, neglects the heterogeneities of individual nodes. The transition rate is usually written as $dX(t)/dt = \alpha X(t)$ where $X(t)$ generically represents a group of nodes being in a possible state X at time t and α is the inverse of the average period a node spent in this state. Under the homogeneous mixing assumption, the infection rate then depends only on the number of individuals in susceptible and infected states, usually given by $\alpha S(t)I(t)$. Such completely random mixing assumption then neglects the actual connections between individuals in a network.

In the recent literature, there are various efforts in extending the classic epidemic models to account for different heterogeneities, as discussed in Sect. "Introduction", since the homogeneous mixing assumption is unrealistic in many real-world applications. This has been highlighted in Pastor-Satorras and Vespignani (2001) when data on virus spread in the Internet, which exhibit power-law degree distribution, are found to be more persistent than that predicted by theoretical results for an homogeneous network. The heterogeneity of connectivity in the network has also been found to potentially cause significantly higher final epidemic prevalence (Leibenzon and Assaf 2024). Building on such results, the more recent work, Johnson (2024) went one step further and argued that the heterogeneity of network structure could be more important than the intrinsic transmissibility of a disease itself and hence, it is important to consider network information into classical epidemic models. In this direction, works such as (Szapudi 2020) and (Volz 2023) proposed to modify the classic SIR model to consider different degree distributions. However, the actual topological structure of the network is not considered in such approach in which we address in our model and this forms one of our contributions.

Besides heterogeneity in terms of connectivity (node degrees), another dimension of heterogeneity relates to the epidemic parameters (*e.g.* transmission and recovery rates). Each node in the network may behave/respond differently to the subject of interest. For instance, Gou and Jin (2017) considered node-specific infection and recovery rates for the classical SIR model and found the basic reproductive number depends on the mean distributions of these rates. In line with this direction, instead of a constant transition rate, several works have proposed to account for the node heterogeneity by modelling the transition rates as a function of an additional parameter. For instance, Berestycki et al. (2023) introduced a risk factor variable to represent that different nodes may have different relative individual vulnerability. On the other hand, Neipel et al. (2020) and Klemm and Ravera (2023) proposed to capture the individuality by introducing a distribution of susceptibilities. In (Govindankutty and Gopalan 2024), the authors extended the *SIS* and *SIR* models to model misinformation spread in digital networks by splitting the infected state into positively and negatively infected (accounting for the possibility of different consequences of infection). In this paper, our model simultaneously considers the above heterogeneities as well as the incubation phase of decision making which has not been explored in similar context and thus, constitute another novelty in our work here. We further refer readers to (Pastor-Satorras et al. 2015) and (de Arruba et al. 2018) for reviews of recent development in modelling epidemic processes.

In this paper, we use as basis the N -Intertwined mean-field approximation (NIMFA) model (or individual-based mean-field) introduced in Van Mieghem et al. (2009), further studied in Van Mieghem (2011) and Sahneh et al. (2013) and extended in Chai and Pavlou (2017), Chai (2018), Sahneh et al. (2012) and Youssef and Scoglio (2011). In this model, a set of ordinary differential equations (ODE) is derived to represent the time evolution of the probability of infection for each individual in a network. The model utilizes an approximation via the application of the mean-field theory which reduce the complexity of the problem and thus, making the approach viable to large networks. Our model accounts for the heterogeneity of connectivity through the inclusion of the (weighted) adjacency matrix representing the exact network topology. Furthermore, it models the heterogeneity of nodes by the possibility to encode specific per node epidemic parameters. Finally, our model extends the SIR model with the additional states of incubation where an attitude (either receptive or resistive) towards adopting the innovation is formed before a decision is made. In short, this paper contributes a novel model on innovation diffusion that concurrently takes into account the role of network structure in innovation adoption spreading, the heterogeneity of individual entity in the network, and also explicitly consider the incubation state in the decision-making process, all under one unified framework based on epidemic modelling.

Model development

We compartmentalize the diffusion process into stages whereby we consider and model an “incubation” period for each node (i.e., from the time of initial exposure of the innovation to the time when an adoption decision is made). Innovation adoption is different from information spreading which is usually classified as a *simple* contagion process (Centola and Macy 2007) where a node is passive (i.e., it is either aware or not of the information) and no actual action is needed. In contrast, innovation adoption is more complex, often requiring multiple and continuous exposure instances. Furthermore, since adoption of an innovation usually involves a decision-making process by the node (or decision through inaction), the node plays an active role (e.g. installing new facilities or software, purchasing new equipment, changing of business processes or operation routine). As such, simply being aware of the existence of an innovation is only the first state and usually an evaluation period ensues before deciding for or against taking up the new innovation. During this period, a node forms its opinion and take up a stance of either being receptive (State A_{rc}) or resistive (State A_{rs}) towards the innovation. Depending on the actual scenario, these temporary stances assumed by nodes prior to making decision can represent either their innate traits or affinities towards new innovations (e.g. collectivist vs individualistic nature, risk-averse vs risk-seeking behaviors, etc.) or their current ability to adopt the innovation.

To offer insights into individual node in a network, we need to consider all combinations of possibilities in the population. The complexity to compute such exact solution has been shown to grow exponentially with the number of nodes in the network (Van Mieghem et al. 2009). We follow the literature (Van Mieghem et al. 2009; Van Mieghem 2011) by applying a mean field approximation and reduce our

problem from exponential to polynomial computational complexity and thus, making our approach scalable to large networks.

In our model, each node in the network is considered to be in one of the five distinct states at any given time as follows:

- Susceptible (State S) – nodes who are yet to be exposed of the innovation (i.e., individual node who are unaware of the new innovation).
- Aware Receptive (State A_{rc}) – nodes who are aware of the innovation, have not decided whether to adopt it and are receptive to the idea of adopting it.
- Aware Resistive (State A_{rs}) – nodes who are aware of the innovation, have not decided whether to adopt it and are resistive to the idea of adopting it.
- Infected (State I) – nodes who have decided to adopt the innovation. We assume the adoption of the innovation by these “infected” nodes are visible by their contacts (or neighbors) and thus, may gain awareness of the innovation.
- Removed (State R) – nodes who have known about the innovation and decided not to adopt. We assume that these nodes do not actively dissuade others from adopting.

Both the A_{rc} and A_{rs} states are temporary and represent the incubation stage for each node before making an adoption decision. As discussed before, these could be characterized by either inherent personality trait of the node or the current state/ability of the node to adopt. For instance, a risk-seeking node may assume a receptive state while an expensive innovation may cause less capable nodes to resist the adoption.

The exact mechanics of the spreading process are as follows:

- A susceptible node can only be infected after coming into contact with an infected node (i.e., an adopter). Ignorant nodes are only exposed to the innovation via adopters. This can be due to them observing the use of innovation by the adopters or the adopters actively communicate this to them. Other exposed nodes who have not made their decisions do not pro-actively spread words regarding the innovation.
- Upon gaining the knowledge of the innovation, a susceptible node assume an initial position which can be receptive or resistive with rate γ_{rc} and γ_{rs} respectively. When considering a population amenable to new innovations, $\gamma_{rc} \gg \gamma_{rs}$ and vice versa. For indifferent or neutral population, $\gamma_{rc} \approx \gamma_{rs}$
- We also allow immediate adoption where a susceptible node decides to adopt at the time of exposure with rate β_0 . Such case usually occurs for the uptake of low-risk low-cost innovation (e.g. using a new free mobile application).
- A receptive (resistive) node adopts the innovation with probability β_{rc} (β_{rs}). This transition is affected by the neighboring adopters.
- A receptive (resistive) node decides against adopting the innovation with probability μ_{rc} (μ_{rs}). Following Van Mieghem et al. (2009), this is assumed to be a Poisson process. Logically, $\beta_{rc} \gg \mu_{rs}$ and $\beta_{rc} \ll \mu_{rs}$.

Figure 1 shows the state transition diagram of our $SA_{rc}A_{rs}IR$ model following the above defined spreading process. It is characterized by the tuple,

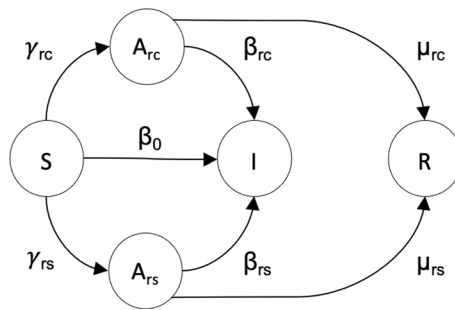


Fig. 1 The $SA_{rc}A_{rs}IR$ model state transition diagram characterized by $H = \{\beta_0, \beta_{rc}, \beta_{rs}, \gamma_{rc}, \gamma_{rs}, \mu_{rc}, \mu_{rs}\}$

$H = \{\beta_0, \beta_{rc}, \beta_{rs}, \gamma_{rc}, \gamma_{rs}, \mu_{rc}, \mu_{rs}\}$ with the conditions $\beta_{rc} \gg \mu_{rc}$ and $\beta_{rs} \ll \mu_{rs}$. In our model, all exposed nodes (i.e., nodes having adopters as their neighbors) eventually decide either to adopt (i.e., assuming state I) or not to adopt (i.e., assuming state R). Unexposed nodes remain in state S .

We consider an underlying undirected network, $\mathcal{G}(\mathcal{V}, \mathcal{E})$ with $\mathcal{V} = \{v_1, \dots, v_N\}$ nodes and $\mathcal{E} = \{e_1, \dots, e_L\}$ links (i.e., the direct contact between two nodes) where their cardinalities, $N = |\mathcal{V}|$ and $L = |\mathcal{E}|$. We represent \mathcal{G} via an adjacency matrix, A , with its elements defined as follows:

$$a_{n,m} = \begin{cases} 1 & \text{if there exists a link between node } n \text{ and node } m \\ 0 & \text{otherwise.} \end{cases}$$

In this work, we consider connected simple networks (i.e., there exists at least one path between any node pair, no self-loops, no multi-edge) and all links are bidirectional (i.e., the relationship between two linked nodes are mutual). For the time being, we will restrict A to be a binary matrix with trace, $tr(A) = \sum_{n=1}^N a_{n,n} = 0$. As such, A is an irreducible non-negative $N \times N$ symmetric matrix. We will discuss the weighted version of A for the heterogeneous case in Sect. "Heterogeneous Innovation Adoption".

Let $s_n(t)$, $a_{rc;n}(t)$, $a_{rs;n}(t)$, $i_n(t)$ and $r_n(t)$ denote the probability of node n being in the susceptible (i.e., unaware), receptive (i.e., aware and inclined to adopt), resistive (i.e., aware and disinclined to adopt), infected (i.e., adopted) and removed (i.e., not adopting) state at time, t , respectively. Since each node must be in one of these five states at any given time, then we have

$$s_n(t) + a_{rc;n}(t) + a_{rs;n}(t) + i_n(t) + r_n(t) = 1 \tag{1}$$

and

$$\frac{ds_n(t)}{dt} + \frac{da_{rc;n}(t)}{dt} + \frac{da_{rs;n}(t)}{dt} + \frac{di_n(t)}{dt} + \frac{dr_n(t)}{dt} = 0. \tag{2}$$

We now apply Markov theory to the entire network. The infinitesimal generator of the system, $Q(t)$, has the dimension of $5^N \times 5^N$. Since we need to account for all the possible permutations of states for each node, the complexity to solve this system of equations

is exponential (i.e., $O(5^N)$). Therefore, computing the solution is only feasible when N is small.

In this work, we approach the problem by considering each node individually. Following this, instead of treating a $Q(t)$ infinitesimal generator with dimension $5^N \times 5^N$, we apply Markov theory to obtain N copies of infinitesimal generator $Q_n(t)$ of the five-state continuous Markov chain for each node separately. We can write the individual infinitesimal generator $Q_n(t)$ of dimension 5×5 as in Equation (3) below:

$$Q_n(t) = \begin{bmatrix} -\sum_{i=2,3,4} q_{1,i;n} & q_{1,2;n} & q_{1,3;n} & q_{1,4;n} & 0 \\ 0 & -(q_{2,4;n} + q_{2,5;n}) & 0 & q_{2,4;n} & q_{2,5;n} \\ 0 & 0 & -(q_{3,4;n} + q_{3,5;n}) & q_{3,4;n} & q_{3,5;n} \\ 0 & 0 & 0 & 0 & 0 \\ 0 & 0 & 0 & 0 & 0 \end{bmatrix} \quad (3)$$

The removed rate is a Poisson process and independent of other nodes' states. Therefore, $q_{2,5;n} = \mu_{rc}$ and $q_{3,5;n} = \mu_{rs}$. In contrast, $q_{1,2;n}$, $q_{1,3;n}$, $q_{1,4;n}$, $q_{2,4;n}$ and $q_{3,4;n}$ are random variables dependent on the activities taking place in other nodes in the network. Specifically, whether a node is exposed to the innovation, assuming a receptive or resistive stance or deciding to adopt an innovation depends on the states of its neighbors and similarly, the states of its neighbors depends on their neighbors' states and so on and so forth. For instance, taking the transition from state S to state A_{rc} , $q_{1,2;n}$ as illustration,

$$q_{1,2;n} = \gamma_{rc} \sum_m^N a_{n,m} \mathbf{1}_{\{X_m(t)=1\}} \quad (4)$$

where $\mathbf{1}_x$ is an indicator function and equals to 1 if event x is true and 0 otherwise. The event $\{X_m(t) = 1\}$, in our case here, is whether node m is infected because only infected (adopting) nodes play a role in exposing/transmitting the innovation to their neighbors. Basically, $q_{1,2;n}$ is a function of the transition rate, γ_{rc} and the states of node n 's neighbors which in turn relates to the adjacency matrix, A . Node n is not susceptible to the innovation until at least one of its neighbors adopts the innovation. Hence, $q_{1,2;n}$ sums all the transition rates of infected neighbors of node m . With the existence of term $\{X_m(t) = 1\}$ in Eq. 4, the state of node m is then coupled with the rest of the nodes in the network.

To proceed with the Markov analysis, the randomness of these variables must be removed (Van Mieghem et al. 2009). One way to account for these dependencies is to condition the relevant elements in Q with all possible combinations of states for all nodes. Unfortunately, this results back to the original problem with the exact Markov chain with exponential complexity.

To address this complexity challenge, we apply a mean field approximation to the abovementioned random variables following the approach discussed in Van Mieghem et al. (2009); Van Mieghem (2011) and use its expected rate instead. Continuing on the illustration above using $q_{1,2;n}$, we then take its average, $E[q_{1,2;n}]$, with $E[\mathbf{1}_x] = Pr[x]$, and obtain the following:

$$E[q_{1,2;n}] = \gamma_{rc} \sum_m^N a_{n,m} Pr[X_m(t) = 1] = \gamma_{rc} \sum_m^N a_{n,m} i_{n,m}(t) \quad (5)$$

Table 1 Expected transition probability

State transition	Expected probability
$S \rightarrow A_{rc}$	$E[q_{1,2;n}] = \gamma_{rc} \sum_{m=1}^N a_{n,m} i_m(t)$
$S \rightarrow A_{rs}$	$E[q_{1,3;n}] = \gamma_{rs} \sum_{m=1}^N a_{n,m} i_m(t)$
$S \rightarrow I$	$E[q_{1,4;n}] = \beta_0 \sum_{m=1}^N a_{n,m} i_m(t)$
$A_{rc} \rightarrow I$	$E[q_{2,4;n}] = \beta_{rc} \sum_{m=1}^N a_{n,m} i_m(t)$
$A_{rs} \rightarrow I$	$E[q_{3,4;n}] = \beta_{rs} \sum_{m=1}^N a_{n,m} i_m(t)$
$A_{rc} \rightarrow R$	$E[q_{2,5;n}] = \mu_{rc}$
$A_{rs} \rightarrow R$	$E[q_{3,5;n}] = \mu_{rs}$

where $E[q_{1,2;n}]$ is a real number and allow us to proceed with the continuous-time Markov theory Van Mieghem (2014). Following the same derivation process, we transform the random variables $q_{1,2;n}$, $q_{1,3;n}$, $q_{1,4;n}$, $q_{2,4;n}$ and $q_{3,4;n}$ to their respective effective rate $E[q_{1,2;n}]$, $E[q_{1,3;n}]$, $E[q_{1,4;n}]$, $E[q_{2,4;n}]$ and $E[q_{3,4;n}]$ which remove the random nature of the state transitions, allowing us to proceed with our analysis with reduced complexity since the complexity of the solution now is reduced from exponential ($O(5^N)$) to polynomial ($O(N)$). Specifically, from the original system of ODEs that has exponential state-space size growth rate, the mean-field approximation allows us to develop a system of non-linear ODEs that linearly grows in state-space with regards to N . For instance, $E[q_{1,4;n}]$ models the effective infection rate of node n . After using mean-field approximation, we summarize the expected probability of the possible state transitions in Table 1.

The corresponding effective infinitesimal generator can now be written as:

$$\overline{Q_n(t)} = \begin{bmatrix} -\sum_{i,i=2,3,4} E[q_{1,i;n}] & E[q_{1,2;n}] & E[q_{1,3;n}] & E[q_{1,4;n}] & 0 \\ 0 & -(E[q_{2,4;n}] + \mu_{rc}) & 0 & E[q_{2,4;n}] & \mu_{rc} \\ 0 & 0 & -(E[q_{3,4;n}] + \mu_{rs}) & E[q_{3,4;n}] & \mu_{rs} \\ 0 & 0 & 0 & 0 & 0 \\ 0 & 0 & 0 & 0 & 0 \end{bmatrix} \tag{6}$$

Applying the Markov differential equation (see Van Mieghem (2014) (10.11) on p. 208), we get the following system of non-linear differential equations,

$$\frac{ds_n(t)}{dt} = -(\beta_0 + \gamma_{rc} + \gamma_{rs})s_n(t) \sum_{m=1}^N a_{n,m} i_m(t) \tag{7}$$

$$\frac{da_{rc;n}(t)}{dt} = \gamma_{rc}s_n(t) \sum_{m=1}^N a_{n,m} i_m(t) - \beta_{rc}a_{rc;n}(t) \sum_{m=1}^N a_{n,m} i_m(t) - \mu_{rc}a_{rc;n}(t) \tag{8}$$

$$\frac{da_{rs;n}(t)}{dt} = \gamma_{rs}s_n(t) \sum_{m=1}^N a_{n,m} i_m(t) - \beta_{rs}a_{rs;n}(t) \sum_{m=1}^N a_{n,m} i_m(t) - \mu_{rs}a_{rs;n}(t) \tag{9}$$

$$\begin{aligned} \frac{di_n(t)}{dt} &= \beta_0 s_n(t) \sum_{m=1}^N a_{n,m} i_m(t) + \beta_{rc} a_{rc;n}(t) \sum_{m=1}^N a_{n,m} i_m(t) + \beta_{rs} a_{rs;n}(t) \sum_{m=1}^N a_{n,m} i_m(t) \\ &= (\beta_0 s_n(t) + \beta_{rc} a_{rc;n}(t) + \beta_{rs} a_{rs;n}(t)) \sum_{m=1}^N a_{n,m} i_m(t) \end{aligned} \tag{10}$$

$$\frac{dr_n(t)}{dt} = \mu_{rc} a_{rc;n}(t) + \mu_{rs} a_{rs;n}(t) \tag{11}$$

Each node obeys the above system of differential equations (i.e., Eqs. 7–11 holds for all nodes $n = 1, \dots, N$). We rewrite the equations in matrix form as below:

$$\frac{dS(t)}{dt} = -(\beta_0 + \gamma_{rc} + \gamma_{rs}) \text{diag}(AI(t))S(t) \tag{12}$$

$$\frac{dA_{rc}(t)}{dt} = \gamma_{rc} \text{diag}(AI(t))S(t) - \beta_{rc} \text{diag}(AI(t))A_{rc}(t) - \mu_{rc} A_{rc}(t) \tag{13}$$

$$\frac{dA_{rs}(t)}{dt} = \gamma_{rs} \text{diag}(AI(t))S(t) - \beta_{rs} \text{diag}(AI(t))A_{rs}(t) - \mu_{rs} A_{rs}(t) \tag{14}$$

$$\frac{dI(t)}{dt} = \beta_0 \text{diag}(AI(t))S(t) + \beta_{rc} \text{diag}(AI(t))A_{rc}(t) + \beta_{rs} \text{diag}(AI(t))A_{rs}(t) \tag{15}$$

$$\frac{dR(t)}{dt} = \mu_{rc} A_{rc}(t) + \mu_{rs} A_{rs}(t) \tag{16}$$

where $S(t) = [s_1(t) \ s_2(t) \ \dots \ s_N(t)]^T$, $A_{rc}(t) = [a_{rc;1}(t) \ a_{rc;2}(t) \ \dots \ a_{rc;N}(t)]^T$, $A_{rs}(t) = [a_{rs;1}(t) \ a_{rs;2}(t) \ \dots \ a_{rs;N}(t)]^T$, $I(t) = [i_1(t) \ i_2(t) \ \dots \ i_N(t)]^T$ and $R(t) = [r_1(t) \ r_2(t) \ \dots \ r_N(t)]^T$. We use $\text{diag}(X(t))$ to denote the diagonal matrix with elements $x_1(t), x_2(t), \dots, x_N(t)$ at the principal diagonal.

We can now solve the above system of equations to obtain the instantaneous evolution of the population for the five distinct states. Furthermore, using Equations (1) and (2), the problem is further reduce from solving $5 \times N$ simultaneous differential equations to $4 \times N$ equations.

For illustration, we create a random topology of size, $N = 100$ (cf. Section "Networks with Different Structural Properties") and using our $SA_{rc}A_{rs}IR$ model developed above, show the evolution of the population in different states over time, t assuming three populations with different attitude to innovation adoption. Specifically, we create the following networks:

- A receptive network – all nodes in the network are more inclined to adopt the new innovation with the tuple setting, $H = \{\beta_0 = 0, \beta_{rc} = 0.9, \beta_{rs} = 0.1, \gamma_{rc} = 0.9, \gamma_{rs} = 0.1, \mu_{rc} = 0.1, \mu_{rs} = 0.9\}$,

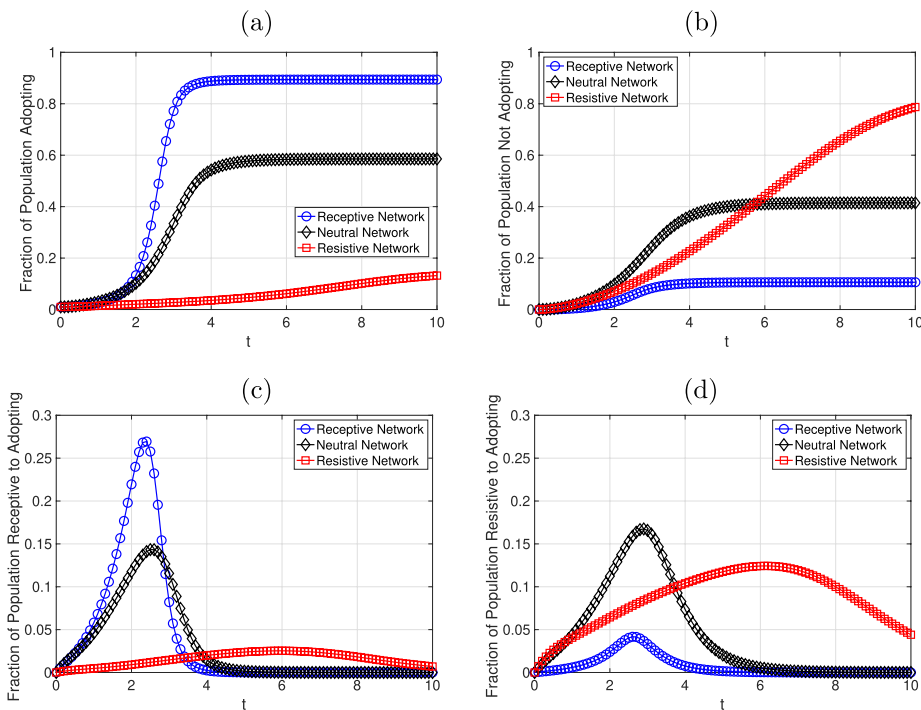


Fig. 2 Instantaneous evolution of the population **a** opting to adopt the innovation, **b** opting not to adopt, **c** in receptive state, and **d** in resistive state for three different networks i.e., receptive (○), neutral (◇), and resistive (□) networks

- A neutral network – all nodes in the network are equally likely to assume a receptive or resistive attitude towards adopting an innovation with the tuple $H = \{\beta_0 = 0, \beta_{rc} = 0.9, \beta_{rs} = 0.1, \gamma_{rc} = 0.5, \gamma_{rs} = 0.5, \mu_{rc} = 0.1, \mu_{rs} = 0.9\}$ and
- A resistive network – all nodes are disinclined to adopt a new innovation with the tuple, $H = \{\beta_0 = 0, \beta_{rc} = 0.9, \beta_{rs} = 0.1, \gamma_{rc} = 0.1, \gamma_{rs} = 0.9, \mu_{rc} = 0.1, \mu_{rs} = 0.9\}$.

Figure 2 shows the model prediction for the three populations in the network generated as described above over time. The receptive network resulted in the highest innovation adoption rate followed by the neutral and then the resistive network. Correspondingly, the population finally decided not to adopt follows the reverse order (i.e., resistive > neutral > receptive networks).

We can compute the fraction of nodes choosing to adopt the innovation at time t in the network using the following:

$$\rho(t) = \frac{1}{N} \sum_{n=1}^N i_n(t). \tag{17}$$

In epidemic terminology, this quantity is analogously known as the epidemic prevalence. Using Eq. (17), the steady state fraction of population adopting the innovation can then be written as:

$$\rho_\infty = \frac{1}{N} \sum_{n=1}^N i_{n\infty} \tag{18}$$

where $i_{n\infty} = \lim_{t \rightarrow \infty} i_n(t)$. It follows also that at steady-state,

$$\sum_n^N s_n + \sum_n^N i_n + \sum_n^N r_n = N \tag{19}$$

since other states are transient and eventually converge to 0 (e.g. $\lim_{t \rightarrow \infty} a_{rc;n}(t) = 0$).

The role of network topology

Recent literature of epidemic has found that insights could be drawn from studying the spectrum of matrix, A , that represents that network topology (Chakrabarti et al. 2007; Van Mieghem et al. 2009; Chai and Pavlou 2017). We follow this line of investigation and derive some properties of the spreading due to the network topologies.

Theorem 1 *Given a fixed tuple $H = \{\beta_0, \beta_{rc}, \beta_{rs}, \gamma_{rc}, \gamma_{rs}, \mu_{rc}, \mu_{rs}\}$, the probability of a node, n , being exposed by the innovation in a network represented by A , is proportional to v_n where v_n is the n -th element of the principal eigenvector corresponding to the largest eigenvalue of matrix, A .*

Proof Since we are considering a connected undirected network, A is irreducible. With this, invoking the Perron-Frobenius theorem, we can choose the principal eigenvector corresponding to the largest eigenvalue, λ_{\max} , to have strictly positive components. By eigen decomposition of A , we get the following:

$$\lambda_{\max}(v_n) = \sum_{m=1}^N a_{n,m} v_n. \tag{20}$$

From Eq. (20), we see that v_n is proportional to the row sum of A . In its canonical form, by analogy with the concept of eigenvector centrality (Wasserman and Faust 1994), matrix A allows us to identify the nodes that are most vulnerable to exposure to a new innovation, i.e., nodes with highest v_n being the ones most prone. □

For a special case of complete graph, we have a symmetric hollow matrix A with $a_{n,m} = 1, \forall n \neq m$ and $a_{n,m} = 0, \forall n = m$. Using this theorem, we can see that all nodes will have the same level of exposure. Under such conditions, we observe that A 's largest eigenvalue, $\lambda_{\max} = (N - 1)a_{n,m}$ while the rest of eigenvalues equal $-a_{n,m}$ with multiplicity $N - 1$. Trivially, the sum of all eigenvalues for this A is zero.

Theorem 2 *Given a fixed tuple, $H = \{\beta_0, \beta_{rc}, \beta_{rs}, \gamma_{rc}, \gamma_{rs}, \mu_{rc}, \mu_{rs}\}$, for any two networks, A and A^* where $0 \leq A \leq A^*$ for which we define $A \leq A^*$ if $a_{n,m} \leq a_{n,m}^* : \forall n, m$, then A^* has higher exposure rate than A .*

Proof We again invoke the Perron-Frobenius theorem that

$$\lambda_{\max}^A \leq \lambda_{\max}^{A^*} \text{ if } 0 \leq A \leq A^* \tag{21}$$

where λ_{\max}^A denotes the largest eigenvalue (or the spectral radius) of A . From Chakrabarti et al. (2007); Gomez et al. (2010); Van Mieghem et al. (2009); Chai and Pavlou (2017), the inverse of spectral radius of the adjacency matrix gives the lower bound estimate of the real epidemic threshold with high accuracy. Following this, by having higher spectral radius, A^* then has higher exposure rate than A . \square

Following Theorem 2, we can then give the following companion theorem:

Theorem 3 *Given two populations characterized respectively with the tuple, $H = \{\beta_0, \beta_{rc}, \beta_{rs}, \gamma_{rc}, \gamma_{rs}, \mu_{rc}, \mu_{rs}\}$ and $H^* = \{\beta_0, \beta_{rc}, \beta_{rs}, \gamma_{rc}^*, \gamma_{rs}^*, \mu_{rc}, \mu_{rs}\}$. For an innovation diffusion in a fixed network, A ,*

$$\rho_{\infty}^H \leq \rho_{\infty}^{H^*} \text{ if } \gamma_{rc} \leq \gamma_{rc}^* \text{ and } \gamma_{rs} \geq \gamma_{rs}^* \tag{22}$$

where ρ_{∞}^H is the steady-state fraction of population adopting the innovation for population characterized by H .

Proof From Theorem 2, we know that the exposure rate would be the same for the two populations since the network topology are the same (i.e., the effect of network topology is isolated). Then, the steady-state adoption rate, ρ_{∞} is dependent on the population characteristic itself which in turn is dependent on γ_{rc} and γ_{rs} (determining if the nodes are either receptive or resistive to adopting new innovations. Correspondingly, conditioned with same $\beta_0, \beta_{rc}, \beta_{rs}, \mu_{rc}$ and μ_{rs} , having higher γ_{rc} and lower γ_{rs} would results in higher ρ_{∞} . \square

Individual node in a network

In this section, we look into the instantaneous evolution of adoption probability of individual node in the network. As prior mentioned, our model consider each node in the network individually in relation its position in the network whereby the network effect is taken into account. Using our model, we can compute the probability of node, n , adopting the innovation, $i_n(t)$.

We show $i_n(t)$ of five randomly chosen nodes (labeled as $n1 - n5$) in a network with $N = 100$ in Fig. 3 using our model with only one seed adopter with $H = \{\beta_0 = 0.1, \beta_{rc} = 0.9, \beta_{rs} = 0.1, \gamma_{rc} = 0.5, \gamma_{rs} = 0.5, \mu_{rc} = 0.1, \mu_{rs} = 0.9\}$ as an illustration.

Nodes $n1, n2$ and $n4$ are two hops away from the seed adopter while the distances from nodes $n3$ and $n5$ to the seed adopter are three and four hops. We can see that being nearer to an adopter offers earlier exposure and simultaneously, the chance of adopting the innovation. One possible application of this observation is to optimize the distances of nodes from the set of seed adopters. However, the distance itself does not necessarily guarantee higher adoption rate as can be seen for nodes $n3$ and $n4$ whereby $n4$ is nearer to the seed adopter but have lower adoption probability. As

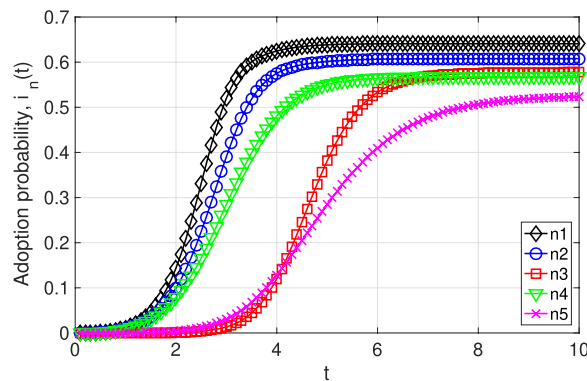


Fig. 3 The adoption probability of five randomly chosen nodes in a sample network

prior discussed, the actual adoption probability is dependent on the position of the node in the network which we will investigate next.

Networks with different structural properties

We proceed to look into the role the network topology plays in the innovation diffusion dynamics. As been found in the literature, network topology structure has strong influences on the actual spreading process. For this, we exploit a range of well-known network models for our study.

The first network model is the Erdős-Rényi (ER) random graph model (Erdős and Rényi 1959). It is one of the most widely used graph models due to its simplicity and tractability properties. ER graphs has binomial degree distribution or a Poisson distribution in the limit of large N . To generate ER networks, a link is randomly created to connect a pair of nodes with probability p_r independent of all other links. To ensure that the network is connected, we set $p_r \geq p_c = \ln(N)/N$. p_c is known as the sharp threshold for connectedness. Unless otherwise stated, we generate our ER networks using $p_r = 2p_c$ to simultaneously ensure a connected network and keeping the link density sufficiently small (link density = $\frac{L}{\binom{N}{2}}$) to avoid a highly meshed topology

(Bornholdt and Schuster 2003).

We also consider the small-world (SW) graph model (Watts and Strogatz 1998). This model reflects the *small-world effect* found in many networks whereby most node pairs are connected by a short path. The small-world effect is said to be present in a network if the mean shortest paths between all node pairs in a network scales logarithmically with N for fixed mean degree. Another important property of SW networks that is different from ER networks is the high network transitivity in SW networks. This means that SW graphs have high number of triangles (i.e., 3 nodes connected to each other directly) – reflecting the phenomenon that a friend of your friend is also likely to be your friend. To generate the SW networks, we follow Newman (2003), starting by creating a uniform lattice topology with all nodes having the same number of neighbors. For each link with probability p , we rewire it to connect to a new pair of nodes. When $p \rightarrow 0$, the resultant network resembles a regular lattice

while when $p \rightarrow 1$, all links are randomly rewired and thus, we get a random graph. For this work, unless explicitly specified otherwise, we set $p = 0.5$. Note also that our method is slightly different from that proposed in Watts and Strogatz (1998) which only rewires one end of the node pair. According to Newman (2003), our method here results in a system that interpolates better between a regular lattice and a random graph.

Finally, scale-free (SF) graph (Barabási and Albert 1999) has been proposed based on observations on many real-world networks (e.g. financial / banking payment networks, airline transportation networks and (online) social networks) exhibiting power-law degree distributions. This means that there are some nodes in the network which has many more direct neighbors than others (i.e., hubs). The presence of hubs is reflected by the long tail in the degree distribution. In generating scale-free networks, we follow Barabási and Albert (1999) where preferential attachment method, also referred to as the *rich get richer* generative model, is used. We begin with one node and in each step, a new node is added with a fixed number of new links, w attached to existing nodes based on the degree of these existing nodes – the higher the degree, the more likely a new node is attached to it. If the number of existing nodes is smaller than w , then the new node is linked to all of them. This results in power-law degree distribution. We use $w = 3$ as default in this work.

We first show the influence of network size on the adoption rate (see Fig. 4). We create a set of ER, SW and SF networks with $N = \{100, 200, 300, 400, 500\}$ where all nodes have no prior preference or prejudice on the innovation by setting the parameters as follows: $\beta_0 = 0.1$, $\beta_{rc} = \mu_{rs} = 0.9$, $\beta_{rs} = \mu_{rc} = 0.1$, $\gamma_{rc} = \gamma_{rs} = 0.5$. We assume a small number of nodes in the network as seed nodes which have adopted the innovation from the beginning. To do this, at time, $t = 0$, a set of ten randomly chosen nodes are set to be in state I . We note that t is dimensionless in our generic case here. It could represent days, months or years depending on the actual scenario being modeled. All other nodes are assumed to be susceptible to exposure of the innovation. When the simulation begins, the seed nodes will start to interact with all their immediate neighbors (i.e., nodes having a direct link to the seed nodes). The spreading process then follow the mechanics described in Sect. "Model development". In the left column of Fig. 4, we show the fraction of population eventually decided to adopt the innovation for an ER, SW and SF network for different network sizes, comparing our model against Monte-carlo simulations. We repeat each experiment 100 times and show the 99% confidence interval in the figures. Our model always predict the adoption rate within the confidence interval. While both SW and SF networks exhibit decreasing adoption rate when N is increased, ER network achieve stable adoption. We conjecture that this is due to the random connections between nodes allow a "uniform" feature across the entire network as oppose to SF, for instance, where many nodes have very few neighbors while a few have disproportionately higher number of neighbors.

We also present the distribution of our results using boxplots in the right column of Fig. 4. The central red line in each box indicates the median and the top and bottom edges of the box represent the 75th and 25th percentiles, respectively. The whiskers extend to the most extreme data points not considered as outliers and finally we plot the outliers individually using the '+' symbol (if any). Each box represents the data computed

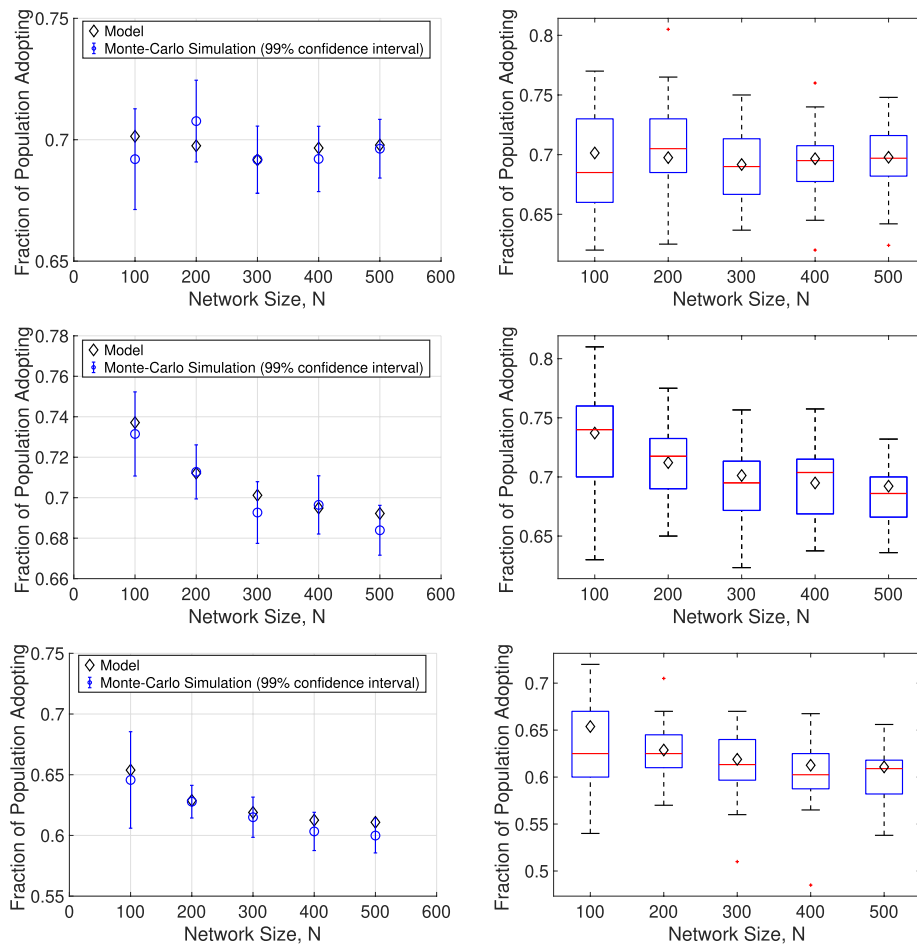


Fig. 4 Predicted fraction (left column) and distribution (right column) of population deciding to adopt the innovation (i.e., “infected” population) in an ER (top row), SW (middle row) and SF (bottom row) network respectively with increasing network size, $N = \{100, 200, 300, 400, 500\}$

over 100 repeated experiments. We use black diamond markers to indicate the predicted result from our $SA_{rc}A_{rs}IR$ model.

Each network model has some parameters we can use to tune the properties of the resulting network. In the following, we investigate one key network generation parameter for each model. Specifically, we use a range of p_c , p and w for ER, SW and SF model respectively with $N = 100$. We show the results in Fig. 5. Similar agreements between our model and experimental results can be observed across the whole spectrum of experiments. Higher p_c for ER and w for SF networks result in increasing adoption rate. These are due to the fact that both parameters lead to higher link density and average degree. This then allow adopters to spread their influence to more individuals. In contrast, we do not observe such phenomenon when changing the p parameter for SW networks. This is because the p parameter in SW only affects the connections between node pairs without changing the actual link density.

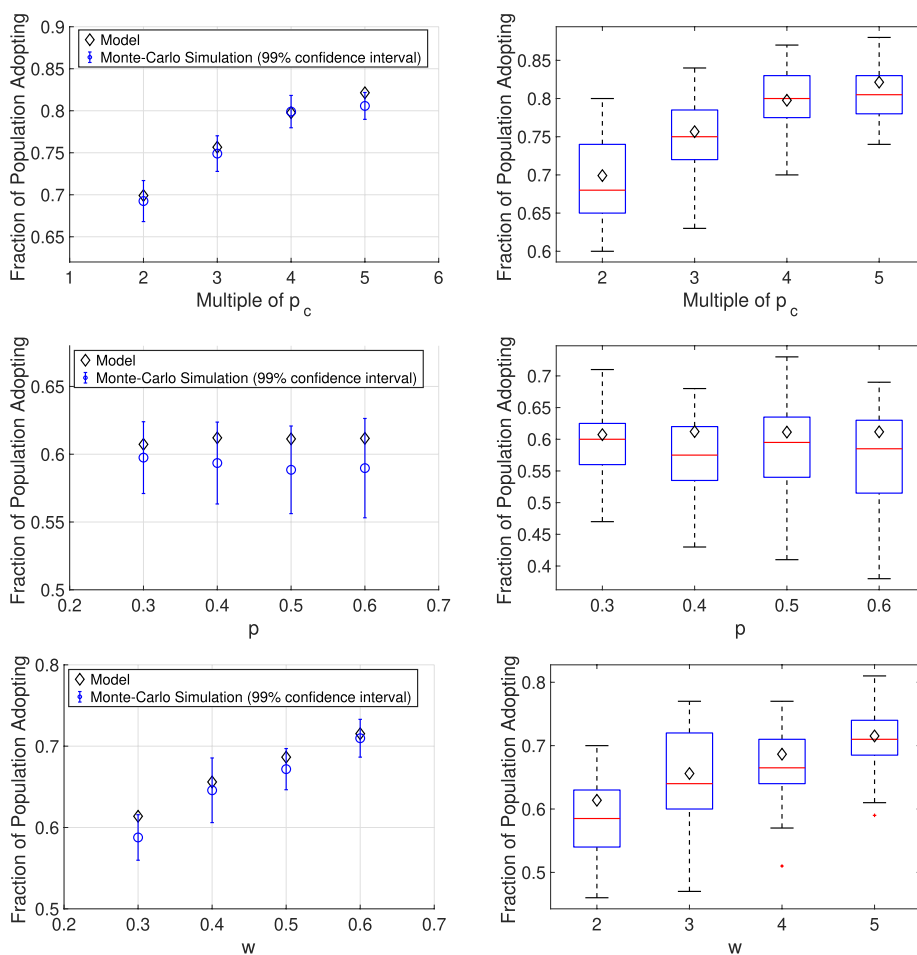


Fig. 5 Predicted fraction (left column) and distribution (right column) of population deciding to adopt the innovation (i.e., “infected” population) in an ER (top row) with $p_c = \{2, 3, 4, 5\}$, SW (middle row) with $p = \{0.3, 0.4, 0.5, 0.6\}$ and SF (bottom row) with $w = \{2, 3, 4, 5\}$ network respectively

Networks with communities

Many real world networks have certain organization components (e.g. geographical component, political boundaries, law barriers, cultural differences) that enforce specific proximity between nodes and play a role in determining which nodes are connected to which. This inherently causes the formation of communities. By community, we mean groups of nodes having high density of links within them and lower link density between the groups. The previous subsection has ignored this aspect, positing the entire network consists of similar individuals.

In this subsection, we investigate how existence of communities in a network affect the adoption of innovations. For this purpose, we leverage the concept of modularity (Newman and Girvan 2004; Newman 2006) which is currently the most used function in determining communities in a network (Fortunato 2010). The basic idea of modularity is that a community has more links between members of the community compared to a randomly formed network. Following Newman and Girvan (2004), modularity of a network, M , can be computed as below:

$$M = \sum_i (e_{ii} - a_i^2), \quad (23)$$

where $a_i = \sum_j e_{ij}$. Further, e_{ij} is the element in a $N \times N$ matrix E , representing the fraction of all edges in the network that link nodes in community i to nodes in community j . Based on the above, a network with high M exhibits strong community structures with low inter-community links and vice versa. Finding the maximum of the modularity metric has been shown to be an NP-complete optimization problem (Brandes et al. 2006). Furthermore, Trajanovski et al. (2013) showed that determining the existence of a graph with prescribed modularity given the number of links and communities is also NP-complete.

Using our $SA_{rc}A_{rs}IR$ model, we study how the existence of communities affect innovation adoption spreading using three representative networks of size, $N = 100$ with three near equal size communities³ but with different $M = \{0.1711, 0.4499, 0.6419\}$ (ranging from weak to strong community features). For comparability, we fixed the same nodes to be in the same community for all the networks (i.e., the first 33 nodes belong to community #1, the next 33 nodes belong to community #2 and the remaining 34 nodes belong to community #3). We use the same default characterization tuple as in Sect. "Networks with different structural properties" and begin with a single random seed node. Using the ER model, we generate random modular networks, retaining near binomial degree distribution characteristic of the network.

We show the result of our model in Fig. 6. The sub-figures in the left column of the figure show the fraction of population of the entire network in different states over time while the sub-figures in the right column show the corresponding adoption and non-adoption rate per community – specifically, curves with markers show the fraction of population in each community choosing to adopt while curves without markers show the fraction of population in each community who choose otherwise. Each row of sub-figures correspond to a network with different community strength, indicated via M (increasing strength from top row to bottom row).

From the figure, we can see that when there is very weak community structure presence (signified by low M value), the adoption spread evolve in the same time manner for all the three groups of nodes. Specifically, we see that the three adoption curves almost overlapped with each other and the same applies to the rejection curves. In the next row, we already can see the three communities make their adoption decision with a "time lag". Finally, we observe in the case where there is strong community structure (third row in the figure), there is clear differentiation between the three communities when the innovation spread across them. For all the cases, the innovation spread the fastest from the community where the seed node belongs. From our results, we can see that existence of communities in a network forms a barrier for an innovation to be diffused across them. However, given time, eventually, the overall innovation adoption rate for each community converge to the similar level. This is because the results here are based on the setting that all communities are homogeneous (i.e., the three communities share the same adoption preferences).

³ We have also experimented with higher number of communities with similar qualitative results.

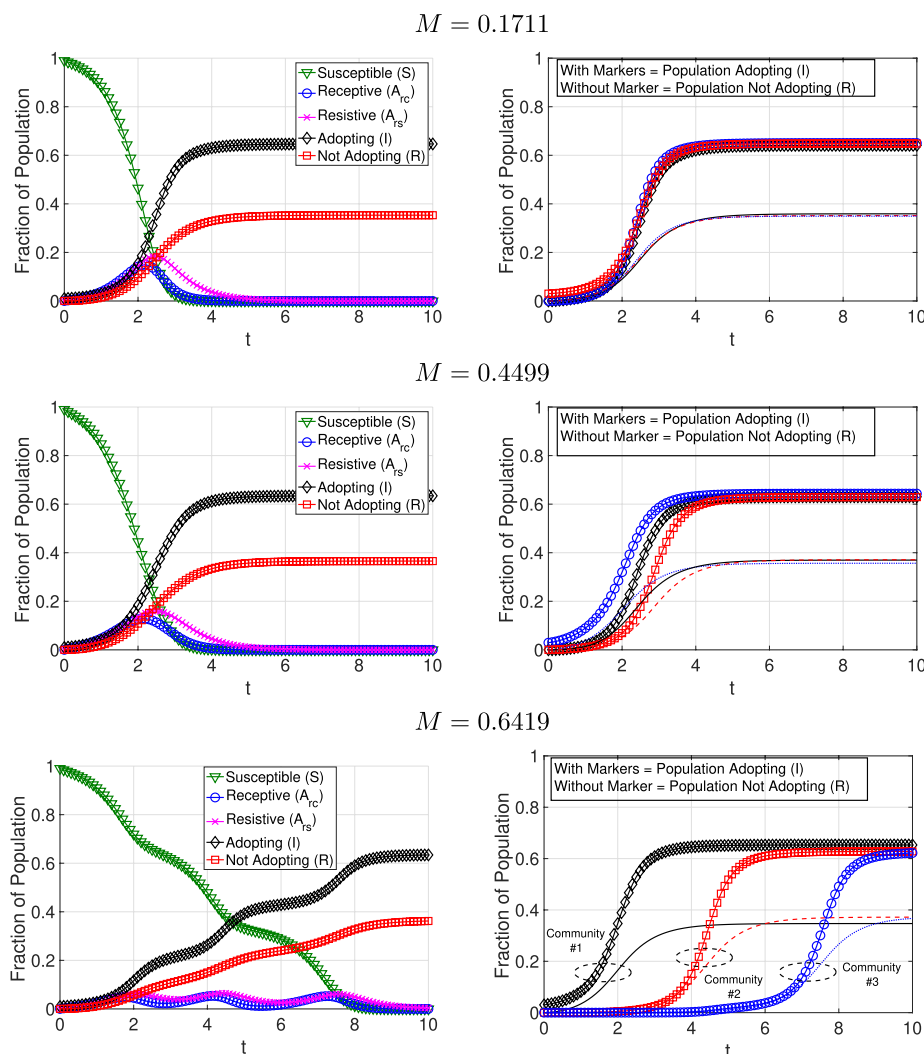


Fig. 6 Innovation adoption spreading in networks with increasing modularity, M , over time, t whereby higher M indicates stronger communities

In Sects. "Networks with different structural properties" and "Networks with communities", we showed how our model can capture the different connectivity features embedded within a network into computing the spreading pattern. As mentioned in Sect. "Model development", our analysis adopts the N -intertwined model (Van Mieghem et al. 2009) which uses individual-based mean-field approximation (MFA). The advantage of this approach is that it keeps the full topological structure of the network encoded in all the entries of the adjacency matrix. Thus, the solutions to individual-based MFA depend on the spectral properties of the adjacency matrix. It assumes that the dynamic state of every node is statistically independent of the state of its nearest neighbors. In this way, our model also capture the modular nature of the input network if there are community structures embedded in the network. This is in contrast to the classical epidemic models (Anderson and May 1991) where homogeneous MFA is employed by assuming that all nodes are the same (i.e., probability of contact between any node pair is

similar). These models have been known to be inaccurate when the network considered is highly irregular and in low dimensions - rendering them ill-suited for modular networks. Another widely used MFA approach in epidemic modelling is degree-based MFA (e.g. Pastor-Satorras and Vespignani (2001), Barrat et al. (2008)) which assumes that all nodes of the same degree are equivalent statistically. Consequently, it implies that the probability of any node with degree k_1 is connected to any node with degree k_2 is the same. In this way, the whole network itself is considered in a mean-field perspective in which the actual topology (i.e., the adjacency matrix) is ignored, only the degree and two-node correlations are preserved (Pastor-Satorras et al. 2015). Again, this approach does not explicitly consider heterogeneity of connections. Adopting individual-based MFA here, we take into account the topological structure of the network (i.e., the skewed distribution of degree as well as different link densities of intra- and inter-community connections are encoded in the model) and thus the embedded community structures are considered. If higher degree of agreement to the exact solution is required, then one can consider higher order approximations. For instance, pair-wise MFA (second-order approximation; sometimes known as Pair Quenched Mean Field (de Arruba et al. 2018)) have been found to offer more accurate performance (Cator and Van Mieghem 2012). In general, higher-order closure techniques can be used to achieve greater accuracy but this is with the cost of much larger state-space size; basically moving back towards the issue of intractability of exact results.

In the next section, we turn our attention from diversity of connectivity to the heterogeneity of infection parameters.

Heterogeneous innovation adoption

In Sect. "Model development", we use the adjacency matrix, A to represent the existence of link between two nodes. With $a_{n,m}$ taking only binary values, A does not encode how strong is the connection between two nodes. In real-world, the strength of connections between two nodes varies. The strength may represent the geographical distance between two nodes, the amount of interactions or how close the relationship between two individuals are. To account for this heterogeneity, we can use a weighted adjacency matrix, W with its elements, $w_{n,m}$, takes the value of the link weight between nodes n and m .

While individual node may share similar preferences and characteristics, in general, the real world is characterized with heterogeneity. To account for this, we now further develop our model described in Sect. "A model for innovation adoption spreading" to account for in-homogeneous nodes in the network. For this purpose, we extend the characterization tuple $H' = \{\beta'_0, \beta'_{rc}, \beta'_{rs}, \gamma'_{rc}, \gamma'_{rs}, \mu'_{rc}, \mu'_{rs}\}$ from constants to a tuple of $N \times 1$ matrices since now each individual node has its own set of tuple. As such, tuple $H'_n = \{\beta'_{0;n}, \beta'_{rc;n}, \beta'_{rs;n}, \gamma'_{rc;n}, \gamma'_{rs;n}, \mu'_{rc;n}, \mu'_{rs;n}\}$ characterizes node n .

Following this, Eqs. 7–11 can be correspondingly extended as below:

$$\frac{dS(t)}{dt} = -\text{diag}(s_n(t)) [W \text{diag}(\beta'_{0;m})I(t) + W \text{diag}(\gamma'_{rc;m})I(t) + W \text{diag}(\gamma'_{rs;m})I(t)] \tag{24}$$

$$\frac{dA_{rc}(t)}{dt} = \text{diag}(s_n(t)) [W \text{diag}(\gamma'_{rc;m}) I(t)] - \text{diag}(a_{rc;n}(t)) [W \text{diag}(\beta'_{rc;m}) I(t) + C] \tag{25}$$

$$\frac{dA_{rs}(t)}{dt} = \text{diag}(s_n(t)) [W \text{diag}(\gamma'_{rs;m}) I(t)] - \text{diag}(a_{rc;n}(t)) [W \text{diag}(\beta'_{rs;m}) I(t) + D] \tag{26}$$

$$\begin{aligned} \frac{dI(t)}{dt} = & \text{diag}(s_n(t)) [W \text{diag}(\beta'_{0;m}) I(t)] + \text{diag}(a_{rc;n}(t)) [W \text{diag}(\beta'_{rc;m}) I(t)] \\ & + \text{diag}(a_{rs;n}(t)) [W \text{diag}(\beta'_{rs;m}) I(t)] \end{aligned} \tag{27}$$

$$\frac{dR(t)}{dt} = \text{diag}(a_{rc;n}(t)) C + \text{diag}(a_{rs;n}(t)) D \tag{28}$$

where $C = [\mu'_{rc;1}, \mu'_{rc;2}, \dots, \mu'_{rc;N}]^T$ and $D = [\mu'_{rs;1}, \mu'_{rs;2}, \dots, \mu'_{rs;N}]^T$.

The system of ODE above now takes into account the unique characteristic of individual node (by extending H with tuple consisting of constants to H' with vectors of transition rates) while at the same time, also, consider the different strength in connections between any two nodes (by using the weighted network representation with W). As such, we consider the nodes to have different traits in innovation adoption and have different connection strengths with each other.

Furthermore, W retains key properties of A . Specifically, W is still a symmetric positive square matrix. The network is weighted and still connected (i.e., one giant component only). Hence, W is also irreducible. With these conditions, for a fixed H' , Theorem 1 and Theorem 2 still apply by replacing A with W .

We can also correspondingly extend Theorem 3 as follows:

Theorem 4 *Given two populations characterized respectively with the tuple, $H' = \{\beta'_0, \beta'_{rc}, \beta'_{rs}, \gamma'_{rc}, \gamma'_{rs}, \mu'_{rc}, \mu'_{rs}\}$ and $H'^* = \{\beta'^*_0, \beta'^*_{rc}, \beta'^*_{rs}, \gamma'^*_{rc}, \gamma'^*_{rs}, \mu'^*_{rc}, \mu'^*_{rs}\}$. For an innovation diffusion in a fixed network, W ,*

$$\rho_\infty^{H'} \leq \rho_\infty^{H'^*} \text{ if } \gamma'_{rc;n} \leq \gamma'^*_{rc;n} \text{ and } \gamma'_{rs;n} \geq \gamma'^*_{rs;n} : \forall n \tag{29}$$

where $\rho_\infty^{H'}$ is the steady-state fraction of population adopting the innovation for population characterized by H' .

Proof The proof trivially follows that of Theorem 3. □

As illustration, we can apply the above heterogeneous version of our model to multilayer network scenario where two or more networks are interconnected. In such context, (1) the intra- and inter-network links often have different characteristics and (2) the nodes in one network may also be different from nodes in another. Consider a two-layer network consisting of G_1 and G_2 represented by an $N_1 \times N_1$ adjacency matrix, A_1 and an $N_2 \times N_2$ adjacency matrix, A_2 respectively where N_x is the size of G_x . The entire topology can then be represented by the following construction of adjacency matrix:

Table 2 Summary on the steps for building of the scenario in the following use cases

Step 1:	Extract trade data from United Nations COMTRADE repository
Step 2:	Set number of nodes for each community (<i>i.e.</i> , country) proportional to total trade volume
Step 3:	Set number of links between community pair (<i>i.e.</i> , country to country links) proportional to total trade volume between the pair.
Step 4:	Construct topology: <ul style="list-style-type: none"> • Create communities based on the number of nodes set in Step 2 • Create links by randomly connecting nodes between two communities based on the number of links set in Step 3
Step 5:	Set epidemic parameters – $\beta_0 = 0.0, \beta_{rc} = \mu_{rs} = 0.9, \beta_{rs} = \mu_{rc} = 0.1$. Both γ_{rc} and γ_{rs} are set based on Table 3 and Table 4 for first and second use case respectively.
Step 6:	Run $SA_{rc}A_{rs}IR$ model.

$$A = \begin{bmatrix} (A_1)_{N_1 \times N_1} & (B)_{N_1 \times N_2} \\ (B^T)_{N_2 \times N_1} & (A_2)_{N_2 \times N_2} \end{bmatrix} \tag{30}$$

where B matrix encodes the interconnection between G_1 and G_2 in which element $b_{n,m} = 1$ if node n in G_1 and node m in G_2 are connected. If there is 1-to-1 mapping between the two network, then $B = I$ where I is the identity matrix. Similar to weighted adjacency matrices, the inter-network links could also be weighted and thus B can equivalently be a weighted matrix and thus, we can get the weighted version of the multi-layer network, W . Such construction can be generally applied to M -layer networks in the following form:

$$W = \begin{bmatrix} W_1 & C_{1,2} & C_{1,3} & \cdots & C_{1,M} \\ (C_{1,2})^T & W_2 & C_{2,3} & \cdots & C_{2,M} \\ (C_{1,3})^T & (C_{2,3})^T & W_3 & \cdots & C_{3,M} \\ \vdots & \vdots & \vdots & \ddots & \vdots \\ (C_{1,M})^T & (C_{2,M})^T & (C_{3,M})^T & \cdots & W_M \end{bmatrix} \tag{31}$$

where W_x is the weighted adjacency matrix of G_x and $C_{y,z}$ is the weighted version of matrix B between G_y and G_z .

Furthermore, to account for the heterogeneity of nodes across different networks (*i.e.*, nodes are homogeneous within the same network but different between networks), we can set the tuple $H'_{n_x} = \{\beta'_{0;n_x}, \beta'_{rc;n_x}, \beta'_{rs;n_x}, \gamma'_{rc;n_x}, \gamma'_{rs;n_x}, \mu'_{rc;n_x}, \mu'_{rs;n_x}\}$ where n_x index the nodes in G_x ; thus differentiating the nodes in each layer. Using the above, we can then apply the set of differential Eqs. 24 – 28 for multilayer networks.

Use cases

We construct two innovation spreading scenarios that consider the heterogeneity in (1) the size of community, (2) the level of interactions between two neighboring communities, and (3) the affinity of each community towards adopting an innovation. Both scenarios are built following the steps summarized in Table 2.

Table 3 Past innovation adoption rates in EU countries (Suriñach and et. al. 2009) as indicators of future affinity to adoption in this use case

Austria	45.2%	Greece	28.4%	Norway	48.2%
Belgium	50.1%	Hungary	30.1%	Portugal	41.0%
Bulgaria	44.5%	Iceland	52.0%	Romania	34.8%
Czech Republic	33.8%	Italy	36.3%	Slovakia	34.3%
Estonia	37.9%	Latvia	36.2%	Spain	41.5%
Finland	41.1%	Lithuania	33.0%	Sweden	36.1%
France	30.1%	Luxembourg	21.2%		
Germany	39.6%	Netherlands	60.7%		

Innovation adoption in the European Union (EU)

A report from Economic and Financial Affairs by the European Commission found that innovation adoption rates are very different amongst European countries even under EU's Single Market Programme (Suriñach and et. al. 2009). We show the reported adoption rates for 22 European countries in Table 3. The adoption rates were computed taking into account different sectors including extractives industry, manufacture industry, electricity, gas and water production and distribution, wholesale and retail trade, transports and communications, financial activities and computer and other business services. They are computed based on two samples extracted from the innovation surveys of the EU (Community Innovation Survey), CIS13 survey, which concerns the innovative activities conducted between 1998 and 2000. The methodology employed follows standard models relying on the use logistic diffusion curve. For this use case, we use the past adoption behavior as indicators of future attitude of the individual node within a country towards adopting a new innovation. As such, we set γ_{rc} and γ_{rs} for each country based on Table 3 (e.g. for Austria, we set $\gamma_{rc:AUT} = 0.452$ and $\gamma_{rs:AUT} = 1 - \gamma_{rc:AUT} = 0.548$; for Belgium, $\gamma_{rc:BEL} = 0.501$ and $\gamma_{rs:BEL} = 0.499$).

In Suriñach and et. al. (2009), it is highlighted that trade and cooperation facilitate innovation spill over from firm to firm and country to country. As such, for constructing the network topology for this use case, we use trade data obtained from the United Nations COMTRADE repository⁴ which offers official international trade data. The trade dataset was extracted for year 2017. For each country, we obtain both the total annual import from and export to another country to represent the bilateral interaction between the two countries. We use the overall country level trade interactions (not industry by industry) by taking the total of all HS commodity codes from the repository. For other search parameters, we use default values from the repository (e.g. Type of product = "Goods", Frequency = "Annual", Modes of Transport = "TOTAL modes of transport", Customs Codes = "TOTAL customs procedure codes"). We use this data as a proxy to represent both the amount of interactions between two countries (the total of import and export for each pair of countries; higher trade involves more interactions and information exchange) and the size of a market in a country. In other words, we set the number of nodes within a country to be proportional to the total trade volume of that market and the link between countries to be proportional to the total import/export

⁴ <https://comtradeplus.un.org/>

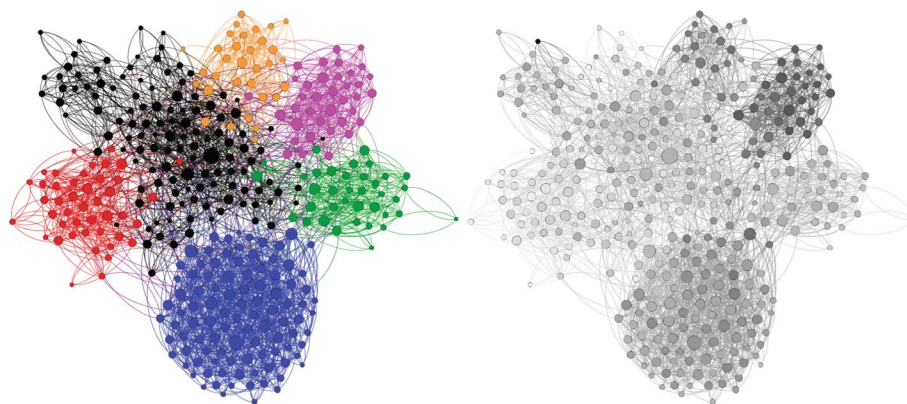


Fig. 7 The constructed network of 22 EU countries based on trade data: (left) The five countries with the largest markets are colored: Germany (Blue), France (Red), Italy (Green), Netherlands (Magenta) and Belgium (Orange); (right) The adoption probability of a node in the network (Darker shade \rightarrow higher adoption probability)

volume between the two markets. In our case, Germany has the highest total trade and thus, we normalize its market size as 1.0 and the size of other markets are all relative to Germany's size (e.g. a market of size 0.5 has half the total trade volume of Germany).

We show in Fig. 7(left) the constructed network topology of size 374 where the five largest markets (i.e., Germany with relative market size \rightarrow 1.0 (100 nodes), France \rightarrow 0.44 (44 nodes), Italy and Netherlands \rightarrow 0.37 (37 nodes each) and Belgium \rightarrow 0.32 (32 nodes)) are highlighted in color. Internally within the country, by extension of the modularity concept, we assume that individual firm within a country has uniform high chances of interacting with each other. Specifically, we represent each country via an ER graph with $p_r = 2p_c$. We use this approximation since understandably there is no available data on actual country-wide detailed business and/or social structure within a market. The final network has a total of 1500 links with 1210 intra-country links and 290 inter-country links. The network results in modularity, $M = 0.6615$ which offers strong community structure.

We apply our $SA_{rc}A_{rs}IR$ model to evaluate an innovation spreading whereby the state transition rate from S to A_{rc} for country, k , $\gamma'_{rc;k}$ is set to the reported adoption rates while its counterpart, $\gamma'_{rs;k}$ is set to $1 - \gamma'_{rc;k}$. In this way, each country has different affinity to adopting a new innovation based on its historical behaviours. Using our $SA_{rc}A_{rs}IR$ model, we compute $i_n(t)$ for the heterogeneous population with node, n , distinctly characterized by $H = \{\beta'_{0;n}, \beta'_{rc;n}, \beta'_{rs;n}, \gamma'_{rc;n}, \gamma'_{rs;n}, \mu'_{rc;n}, \mu'_{rs;n}\}$. We show the result in Fig. 7(right) where we use a greyscale gradient color to indicate the adoption probability of each node (i.e., higher adoption probability is indicated by darker shade and vice versa). We see that nodes within Netherlands (magenta nodes in Fig. 7(left)) have the highest adoption rate while nodes within France (red nodes in Fig. 7(left)) are expected to have low adoption rate despite having the second largest adoption index as input. Furthermore, we also observe that nodes with similar adoption tuple may have different adoption probabilities – e.g. Germany (blue nodes) has varied adoption rates for the constituent nodes - highlighting the impact of topology structure in influencing the spreading dynamics.

We show in Fig. 8a the aggregated adoption rate over time for the 22 EU countries. The innovation achieves 45.62% adoption. When compared to the adoption behaviours exhibited in theoretical graph models, the exposure and subsequently the decision-making process are much slower. We further delve into the adoption behaviours of individual country. We show in Fig. 8b the adoption rates of individual country over time with one random pioneer adopter as seed. We additionally included 8c which only show a subset of the individual countries from Fig. 8b for clearer presentation. We see that the adoption rate differs for each country as opposed to the homogeneous community-less case where adoption rates are almost similar (see Fig. 6 (top right) with overlapping curves). The Netherlands achieves the highest adoption rate at 61.33% (14.81% higher than the aggregate adoption rate). Conversely, France has the lowest adoption rate at 37.48% (i.e., 9.04% lower than the aggregate rate). Netherlands and Belgium who are reported to be receptive of new innovations are predicted to achieve high adoption rates. However, Iceland, Norway and Austria are expected to have lower adoption level than Germany and Spain even though they are reported to have a more resistive attitude. This again show the influence of network structure on the adoption pattern.

Finally, we conducted a series of Monte-Carlo experiments for comparison with our $SA_{rc}A_{rs}IR$ model. We present the results in Fig. 9 which matches well the model prediction (black diamond markers \diamond) and the distribution of the results over 300 repeated experiments. Unlike the homogeneous cases, there are cases where the diffusion instances that take very different paths from the prediction (i.e., more outliers). For Iceland, due to the small total trade volume, it is only represented by one node in the network and thus, the median from the Monte-Carlo experiment is 1.0 but having wide distribution (distributed over 0.0 and 1.0). In general, the interquartile range (IQR) is narrower for countries with larger market size (i.e., more nodes in the network) and vice versa. However, on average, $SA_{rc}A_{rs}IR$ manages to predict the adoption rate within the IQR.

Adoption of financial technologies (Fintech) in the world

We focused previously on adoption for nodes operating in the same environment (i.e., EU countries in the Single Market Programme). Here, we investigate the adoption of specific category of innovation – financial technologies (Fintech). We follow the same process of scenario construction given in Table 2 and use the Fintech adoption index computed by Ernst & Young (Gulamhuseinwala and et. al. 2017) in which 17 distinct services offered by FinTech organizations and non-traditional providers are considered and classified into five broad service categories, namely money transfer and payments, financial planning, savings and investments, borrowing, and insurance. The report considered an individual who has used more than one FinTech services within the last six months as a regular FinTech user. The report is based on 22,000 online interviews across 20 markets (countries). The surveyed population is demographically representative sample of each market. The report applied unweighted averaging of results, i.e., all markets have equal weighting. We show the reported Fintech adoption index in Table 4 for the 20 countries considered in this report.

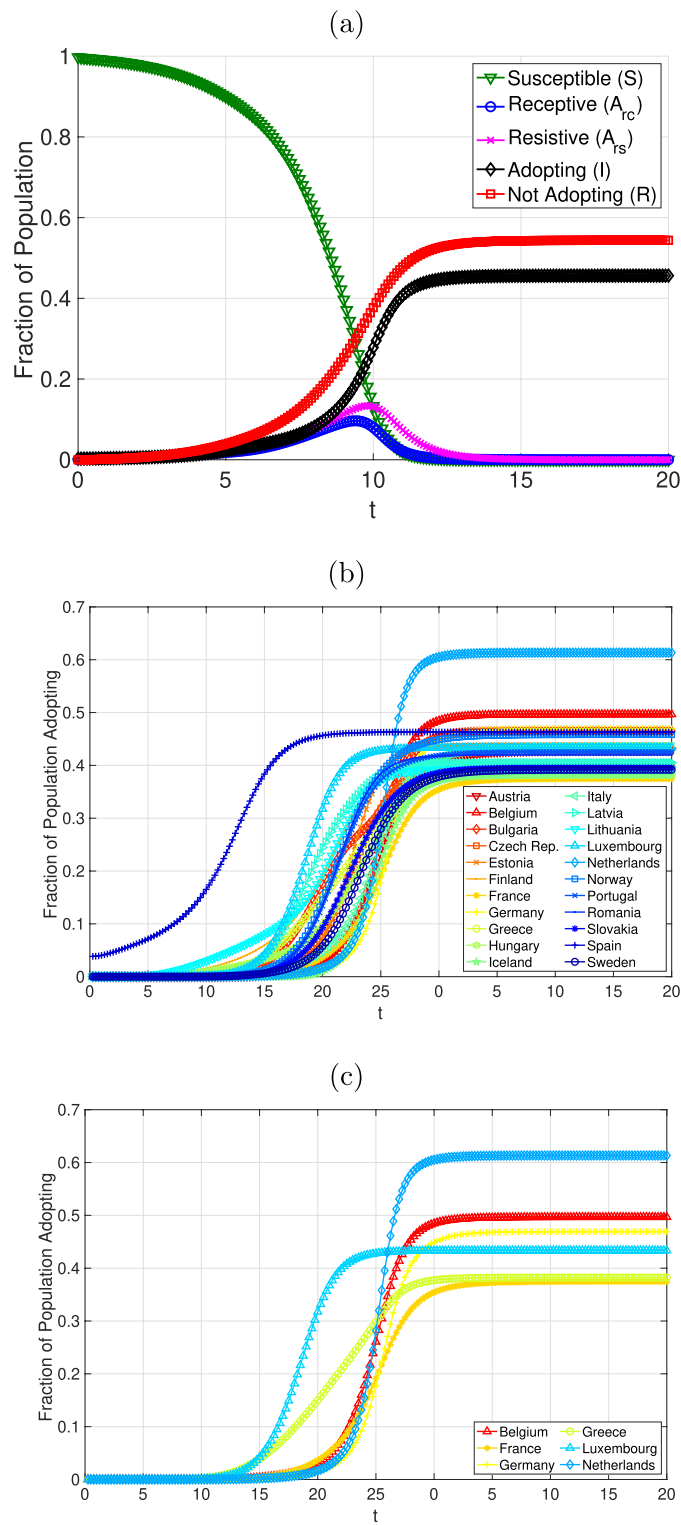


Fig. 8 Aggregated and individual adoption rates for 22 EU countries over time: **a** aggregated; **b** individual country (all); **c** subset of individual countries for clearer presentation

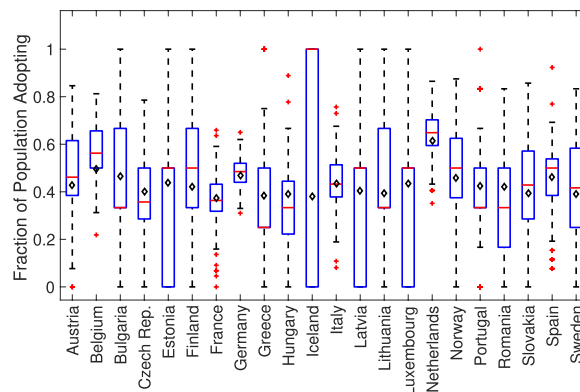


Fig. 9 Fraction of population in different countries adopting the innovation: $SA_{rc}A_{rs}IR \rightarrow$ Diamond markers and Monte-Carlo results \rightarrow Boxplot

Table 4 Fintech adoption Index (Gulamhuseinwala and et. al. 2017)

Australia	37%	Hong Kong	32%	South Africa	35%
Belgium & Luxembourg	13%	India	52%	South Korea	32%
Brazil	40%	Ireland	26%	Spain	37%
Canada	18%	Japan	14%	Switzerland	30%
China	69%	Mexico	36%	UK	42%
France	27%	Netherlands	27%	USA	33%
Germany	35%	Singapore	23%		

Following the rationale and methodology detailed in Sect. "Innovation adoption in the European Union (EU)", we construct the topology for the 20 countries in the index list using COMTRADE data, resulting in a network with $N = 590$ (e.g. China with the largest relative market size \rightarrow 100 nodes, USA \rightarrow 97 nodes, Germany \rightarrow 64 nodes, Japan \rightarrow 34 nodes and both Hong Kong and France \rightarrow 28 nodes each) and $L = 2357$ (2115 intra-country links, 242 inter-country links). We show the topology in Fig. 10(left) with the six largest markets, namely China (relative market size = 1.0), USA (0.97), Germany (0.64), Japan (0.34), France (0.28) and Hong Kong (0.28), highlighted. While previous use case has one large market (i.e., Germany) and most others having much smaller market size, in this case, there are two large markets of almost equal size (i.e., China and USA) with others having comparatively higher market sizes than the previous one.

With our individualized approach, we show the expected adoption rate for every node in the network in Fig. 10(right). From the figure, we see that nodes in the China cluster have high Fintech adoption rate (blue nodes in Fig. 10(left)). This matches intuitively since China has the highest Fintech adoption index. Conversely, Japan (magenta nodes in Fig. 10(left)) is the most resistive nation as we observe that nodes in the Japan cluster have low adoption rates. Furthermore, we see several nodes in the USA cluster (red nodes in Fig. 10(left)) have significantly higher adoption rates than others in the same cluster. These nodes are at the edge of the USA cluster and have direct links to China which is highly receptive. Hence, nodes from the same country (homogeneous within the country) can, in the end, have different adoption

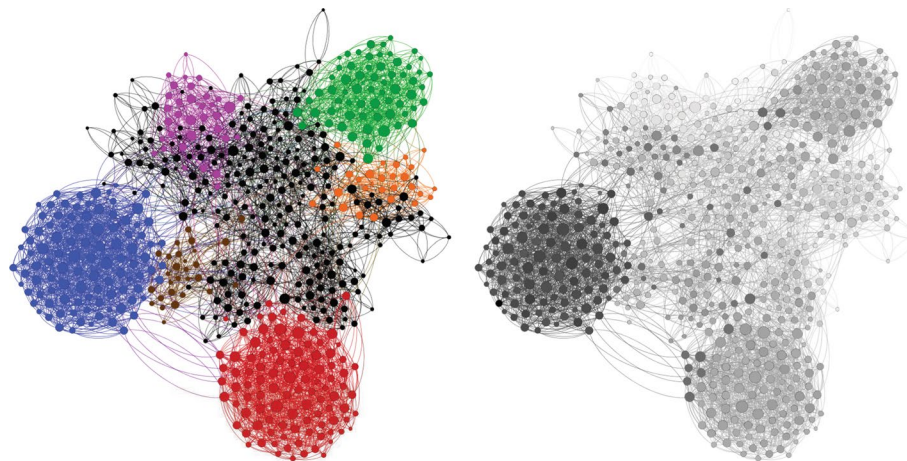


Fig. 10 The constructed network of 20 countries based on trade data: (left) The six largest markets are colored: China (Blue), USA (Red), Germany (Green), Japan (Magenta), France (Orange), and Hong Kong (Brown); (right) The adoption probability of a node in the network (Darker shade \rightarrow higher adoption probability)

probabilities due to the heterogeneity of connections (i.e., the impact of topological structure on the final adoption). Similarly, another illustration of this effect pertains to the left edge of Germany (green nodes) in the figure where 3 nodes visibly have higher adoption probability than other green nodes.

We show in Fig. 11a the aggregated Fintech adoption rate for the 20 countries in the Fintech adoption index. The network's modularity, $M = 0.7837$ which has stronger community structure than the previous use case. This feature can be seen in this figure with multiple peaks on the receptive and resistive population (similar to the left bottom subfigure in Fig. 6). At this aggregated level, the adoption rate is computed at 44.21%.

We show the time evolution of adoption rates for each country in Fig. 11b. For better presentation, we selected a subset of the individual countries and additionally presented them in Fig. 11c. China who has been found to be highly receptive in adopting Fintech innovations are expected to have high adoption rate at 71.73% (27.52% higher than the aggregate rate). Conversely, Belgium and Luxembourg has the lowest adoption rate at 26.09% (18.12% lower than the aggregate rate). These corresponds well with their Fintech adoption index. However, Brazil with 4th highest index is only computed to reach adoption rate of 39.92% (ranked 10th in the predicted adoption rate).

We proceed to show the results of 300 repeated Monte-Carlo experiments in Fig. 12. One random seed adopter is set at the start of each experiment. In general and in agreement with Van Mieghem et al. (2009), Monte-Carlo simulations produce larger deviations for smaller communities and vice versa. Nevertheless, the experiment results follow the computed output of our $SA_{rc}A_{rs}IR$ model.

Conclusions

In this paper, we developed a scalable, tractable and general model for predicting innovation diffusion. It simultaneously takes into account the structure of the social/business contact network of the stakeholders as well as their individual adoption trait. Methodologically, we extend the latest epidemic theory and proposed the $SA_{rc}A_{rs}IR$ model

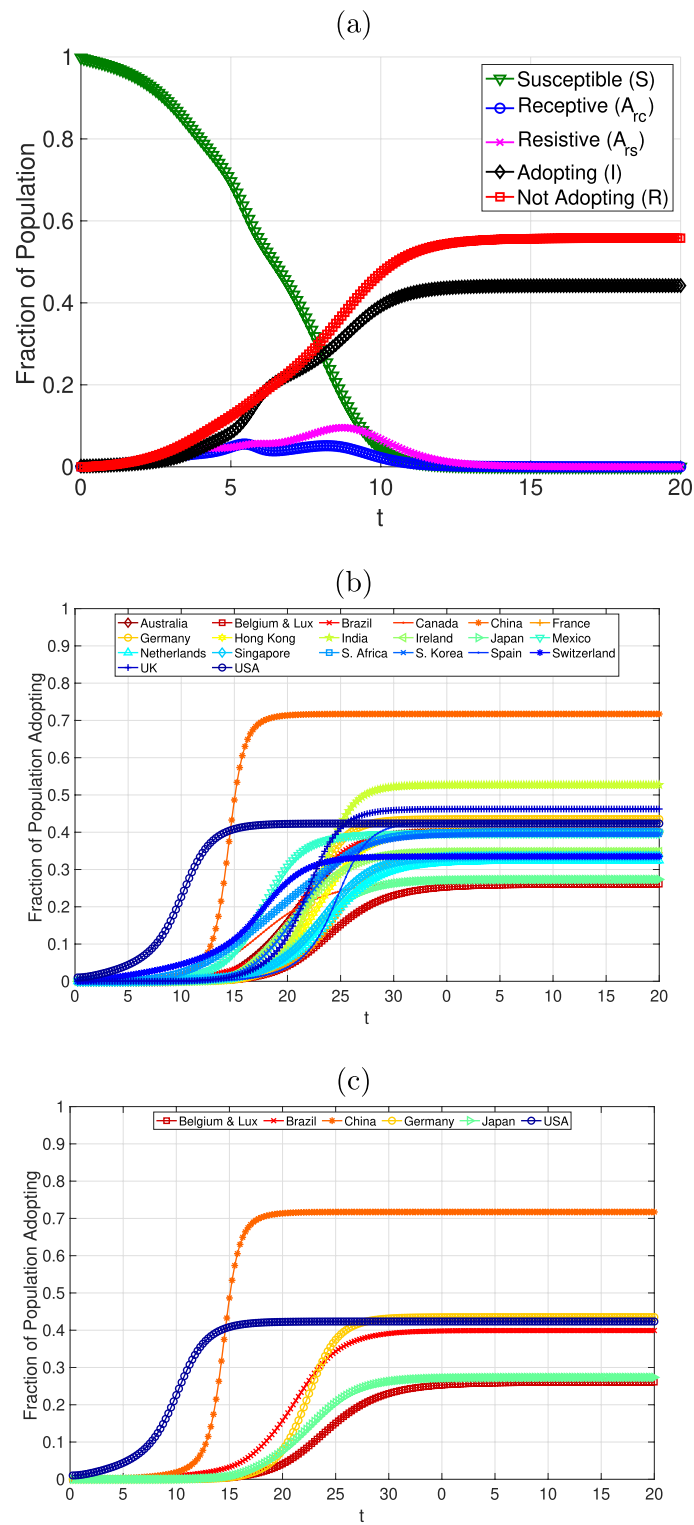


Fig. 11 Aggregated and individual Fintech adoption rates for 20 countries over time: **a** aggregated; **b** individual country (all); **c** subset of individual countries for clearer presentation

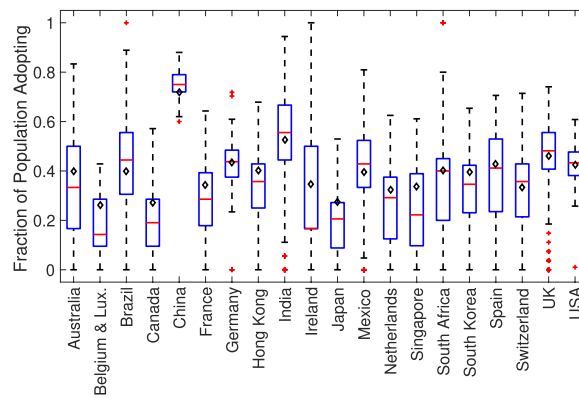


Fig. 12 Fraction of population in different countries adopting Fintech: $SA_{IC}A_{IS}/R \rightarrow$ Diamond markers and Monte-Carlo results \rightarrow Boxplot

which specifically models an incubation stage whereby once an individual in the network learned about the new innovation, it forms an initial opinion (either being receptive or resistive) regarding the innovation before proceeding to make an adoption decision.

We show that the time to get exposure of the innovation is related to position of the individual in relation with other adopters in the network. However, we found that time to exposure and adoption rate are not necessarily correlated as the individual node’s adoption behaviour also plays an important role. Moreover, a positive adoption decision is related to the number of neighbors adopting the innovation. The neighbors decisions are, in turn, dependent on their own neighbors and so, it forms a complex cascading inter-dependent relationship between the different individuals in the network. As such, each node in the network is unique and its relevant adoption rate must be considered separately conditioned with the activities occurring in the network over time. Our approach exactly allows us to compute individual adoption probability.

We consider both homogeneous (i.e., all nodes possess similar adoption behaviours) and heterogeneous (i.e., nodes have different traits in innovation adoption and have different connection strengths with each other) populations. For the homogeneous population, we study our model via the use of three network models (including random, small-world and scale-free networks) complemented with random modular networks exploiting the concept of modularity to include the effect of social community structures in the network. For the heterogeneous case, we extend the model using weighted network representation to account for different level of interactions between nodes and individualized set of state transition probabilities to account for the unique character of each node. Our model is sufficiently general to allow study of different network structures resulted from any information systems and effect of other interesting factors (e.g. homophilic tendencies of population) that may dictate diffusion paths. We illustrated the effects of the embedded social structure in digital networks via two use cases – (i) innovation adoption of EU countries in a Single Market Programme and (ii) innovation adoption of specific class of technology (specifically financial technologies).

Author contributions

The authors contributed equally to this work.

Data Availability

Trade data obtained from <https://comtradeplus.un.org/> is used in the use cases.

Declarations**Competing interests**

The authors declare no competing interests.

Received: 9 December 2024 Accepted: 28 February 2025

Published online: 09 April 2025

References

- Acemoglu D, Antràs P, Helpman E (2007) Contracts and technology adoption. *Am Econ Rev* 97(3):916–943
- Acemoglu D, Ozdaglar A, Yildiz E (2011) Diffusion of innovations in social networks. *IEEE Conf on Decision and Control and European Control* pp 2329–2334
- Ambrus A, Mobius M, Szeidl A (2014) Consumption risk-sharing in social networks. *Am Econ Rev* 104(1):149–182
- Anderson RM, May RM (1991) *Infectious diseases of humans*. Oxford University Press
- de Arruba GF, Rodrigues FA, Moreno Y (2018) Fundamentals of spreading processes in single and multilayer complex networks. *Phys Rep* 756:1–59
- Bandiera O, Rasul I (2006) Social networks and technology adoption in northern mozambique. *Econ J* 116:869–902
- Banerjee A, Chandrasekhar A, Dufló E, et al (2013) The diffusion of microfinance. *Science* 341
- Barabási AL, Albert R (1999) Emergence of scaling in random networks. *Science* 286(5439):509–512
- Barrat A, Barthélemy M, Vespignani A (2008) *Dynamical processes on complex networks*. Cambridge University Press
- Berestycki H, Desjardins B, Weitz JS et al (2023) Epidemic modeling with heterogeneity and social diffusion. *J Math Biol* 86:60
- Bhattacharya K, Mukherjee G, Saramaki J, et al (2008) The international trade network: weighted network analysis and modelling. *J Stat Mech* P02002
- Borge-Holthoefer J, Baños RA, González-Bailón S et al (2013) Cascading behaviour in complex socio-technical networks. *J Complex Netw* 1:3–24
- Bornholdt S, Schuster HG (2003) *Handbook of graphs and networks*. Wiley
- Brandes U, Delling D, Gaertler M et al (2006) On modularity - np-completeness and beyond. Karlsruhe Univ, Fak für Informatik, Bibliothek
- Cator E, Van Mieghem P (2012) Second-order mean-field susceptible-infected-susceptible epidemic threshold. *Phys Rev E* 85(5):056111
- Centola D, Macy M (2007) Complex contagions and the weakness of long ties. *Am J Sociol* 113(3):702–734
- Chai WK (2018) Modelling spreading process induced by agent mobility in complex networks. *IEEE Trans Netw Sci Eng* 5(4):336–349
- Chai WK, Pavlou G (2017) Path-based epidemic spreading in networks. *IEEE/ACM Trans Netw* 25(1):565–578
- Chakrabarti D, Leskovec J, Faloutsos C, et al (2007) Information survival threshold in sensor and p2p networks. *IEEE Int'l Conf Comp Commun (INFOCOM)* pp 1316–1324
- Chen W, Kamal F (2016) The impact of information and communication technology adoption on multinational firm boundary decisions. *J Int Bus Stud* 47:563–576
- Daley DJ, Gani J (1999) *Epidemic modelling: an introduction*. Cambridge University Press
- Delre S, Jager W, Janssen M (2007) Diffusion dynamics in small-world networks with heterogeneous consumers. *Comput Math Organiz Theor* 13:185–202
- Dinh T, Zhang H, Nguyen D et al (2014) Cost-effective viral marketing for time-critical campaigns in large-scale social networks. *IEEE/ACM Trans Netw* 22(6):2001–2011
- Dreiling M, Darves D (2011) Corporate unity in American trade policy: a network analysis of corporate-dyad political action. *Am J Sociol* 116(5):1514–1563
- Duernecker G, Vega-Redondo F (2018) Social networks and the process of globalization. *Rev Econ Stud* 85(3):1716–1751
- Erdős P, Rényi A (1959) On random graphs, I. *Publicationes Mathematicae (Debrecen)* 6:290–297
- Fogli A, Veldkamp L (2012) Germs, social networks and growth. Working Paper 18470, National Bureau of Economic Research. <https://doi.org/10.3386/w18470>, <http://www.nber.org/papers/w18470>
- Fortunato S (2010) Community detection in graphs. *Elsevier Phys Rep* 486(3–5):75–174
- Garetto M, Gong W, Towsley D (2003) Modeling malware spreading dynamics. *IEEE Int'l Conf Comp Commun (INFOCOM)* 3:1869–1879
- Giordano G, Blanchini F, Bruno R et al (2020) Modelling the covid-19 epidemic and implementation of population-wide interventions in italy. *Nat Med* 26:855–860
- Gomez S, Arenas A, Meloni Borge-Holthoefer SJ, et al (2010) Discrete time markov chain approach to contact-based disease spreading in complex networks. *Europhys Lett* 89:38009
- Gou W, Jin Z (2017) How heterogeneous susceptibility and recovery rates affect the spread of epidemics on networks. *Infect Dis Model* 2(3):353–367
- Govindankutty S, Gopalan SP (2024) Epidemic modeling for misinformation spread in digital networks through social intelligence approach. *Sci Rep* 14:19100
- Granovetter M (1978) Threshold models of collective behavior. *Am J Sociol* 83(6):1420–1443
- Gulamhuseinwala I, et. al. (2017) EY FinTech Adoption Index 2017: The rapid emergence of FinTech. Ernst & Young Global

- Hofstede G (2003) Culture's consequences: comparing values, behaviors, institutions and organizations across nations. SAGE Publications Inc
- Jackson MO, Lopez-Pintado D (2013) Diffusion and contagion in networks with heterogeneous agents and homophily. *Netw Sci* 1(1):49–67
- Johnson S (2024) Epidemic modelling requires knowledge of the social network. *J Phys Complex* 5:01LT01
- Kali R, Reyes J (2007) The architecture of globalization: a network approach to international economic integration. *J Int Bus Stud* 38:595–620
- Kephart JO, White SR (1993) Measuring and modelling computer virus prevalence. *IEEE Symposium on Security and Privacy*
- Kermack WO, McKendrick AG (1927) A contribution to the mathematical theory of epidemics. *Proc Roy Soc London Ser A* 115(772):700–721
- Kim S, Shin EH (2002) A longitudinal analysis of globalization and regionalization in international trade: a social network approach. *Soc Forces* 81(2):445–471
- Kinne JB (2012) Multilateral trade and militarized conflict: centrality, openness, and asymmetry in the global trade network. *J Polit* 74(1):308–322
- Klemm S, Ravera L (2023) On sir-type epidemiological models and population heterogeneity effects. *Physica A: Stat Mech Appl* 624:128928
- Koka BR, Prescott JE, Madhavan R (1999) Contagion influence on trade and investment policy: a network perspective. *J Int Bus Stud* 30(1):127–147
- Leibenzon A, Assaf M (2024) Heterogeneity can markedly increase final outbreak size in the sir model of epidemics. *Phys Rev Res* 6:L012010
- Li H, Cheng X, Liu J (2014) Understanding video sharing propagation in social networks: measurement and analysis. *ACM Trans Multimedia Comput Commun Appl* 10(4):33:1–33:20
- Liu Z, Magal P, Seydi O et al (2020) A covid-19 epidemic model with latency period. *Infect Dis Model* 5:323–337
- Mili L, Rossetti G, Pedreschi D, et al (2018) Active and passive diffusion processes in complex networks. *Appl Netw Sci* 3(42)
- Morris MW, Yy Hong, Cy Chiu et al (2015) Normology: integrating insights about social norms to understand cultural dynamics. *Organ Behav Hum Decis Process* 129:1–13
- Neipel J, Bauermann J, Harmon T et al (2020) Power-law population heterogeneity governs epidemic waves. *PLoS One* 15:e0239678
- Newman MEJ (2003) The structure and function of complex networks. *SIAM Rev* 45(2):167–256
- Newman MEJ (2006) Finding community structure in networks using the eigenvectors of matrices. *Phys Rev E* 74:036104
- Newman MEJ, Girvan M (2004) Finding and evaluating community structure in networks. *Phys Rev E* 69:026113
- Olcina G, Panebianco F, Zenou Y (2018) Conformism, social norms and the dynamics of assimilation. *IZA Discussion Paper* 11436
- Pastor-Satorras R, Vespignani A (2001) Epidemic spreading in scale-free networks. *Phys Rev Lett* 86:3200–3203
- Pastor-Satorras R, Castellano C, Van Mieghem P et al (2015) Epidemic processes in complex networks. *Rev Mod Phys* 87:925–979
- Rogers EM (2003) Diffusion of innovations. *Simon & Schuster Int'l*
- Sahneh F, Chowdhury FN, Scoglio C (2012) On the existence of a threshold for preventive behavioral responses to suppress epidemic spreading. *Sci Rep* 2:632
- Sahneh F, Scoglio C, Van Mieghem P (2013) Generalized epidemic mean-field model for spreading processes over multilayer complex networks. *IEEE/ACM Trans Netw* 21(5):1609–1620
- Suriñach J, et al (2009) The diffusion/adoption of innovation in the internal market. *European Economy Economic Papers*
- Szapudi I (2020) Heterogeneity in sir epidemics modeling: superspreaders and herd immunity. *Appl Netw Sci* 5(1):93
- Tinn K (2010) Technology adoption with exit in imperfectly informed equity markets. *Am Econ Rev* 100:925–957
- Trajanovski S, Kuiper FA, Martín-Hernández J et al (2013) Generating graphs that approach a prescribed modularity. *Comput Commun* 36:363–372
- Van Mieghem P (2011) The n-intertwined sis epidemic network model. *Computing* 93(2):147–169
- Van Mieghem P (2014) Performance analysis of complex networks and systems. Cambridge University Press
- Van Mieghem P, Omic J, Kooij R (2009) Virus spread in networks. *IEEE/ACM Trans Netw* 17(1):1–14
- Vojnović M, Gupta V, Karagiannis T et al (2010) Sampling strategies for epidemic-style information dissemination. *IEEE/ACM Trans Netw* 18(4):1013–1025
- Volz E (2023) Sir dynamics in random networks with heterogeneous connectivity. *Journ Math Biol* 56(3):293–310
- Wasserman S, Faust K (1994) *Social Network Analysis: Methods and Applications*. Cambridge University Press
- Watts DJ, Strogatz SH (1998) Collective dynamics of 'small-world' networks. *Nature* 393(6684):440–442
- Whittle P (1955) The outcome of a stochastic epidemic - a note on bailey's paper. *Biometrika* 42:116–122
- Young P (2003) The diffusion of innovations in social networks. In: *The Economy as a Complex Evolving System, Vol. III*. Oxford University Press
- Young P, Burke M (2001) Competition and custom in economic contracts: a case study of illinois agriculture. *Am Econ Rev* 91(3):559–573
- Youssef M, Scoglio C (2011) An individual-based approach to sir epidemics in contact networks. *J Theor Biol* 283(1):136–144

Publisher's Note

Springer Nature remains neutral with regard to jurisdictional claims in published maps and institutional affiliations.